

# **DNA oxidation induced by fetal exposure to BPA agonists impairs female meiosis.**

Sonia Abdallah<sup>1</sup>, Delphine Moison<sup>1</sup>, Margaux Wieckowski<sup>1</sup>, Sébastien Messiaen<sup>1</sup>, Emmanuelle Martini<sup>1</sup>, Anna Campalans<sup>2</sup>, J. Pablo Radicella<sup>2</sup>, René Habert<sup>1</sup>, Gabriel Livera<sup>1\*</sup>, Virginie Rouiller-Fabre<sup>1</sup>, Marie-Justine Guerquin<sup>1\*</sup>.

<sup>1</sup> Laboratory of Development of the Gonads, UMRE008 Genetic Stability Stem cells and Radiations, Université de Paris, Université Paris Saclay, CEA/DRF/IBFJ/IRCM, F-92265 Fontenay aux Roses, France.

<sup>2</sup> Laboratory of Genetic Instability Research, UMRE008 Genetic Stability Stem cells and Radiations, Université de Paris, Université Paris Saclay, CEA/DRF/IBFJ/IRCM, F-92265 Fontenay aux Roses, France.

\* **Correspondences:** [marie-justine.guerquin@cea.fr](mailto:marie-justine.guerquin@cea.fr), [gabriel.livera@cea.fr](mailto:gabriel.livera@cea.fr)

*Further information and requests for resources and reagents should be directed to and will be fulfilled by the Lead contact, [marie-justine.guerquin@cea.fr](mailto:marie-justine.guerquin@cea.fr).*

## 14 **Summary**

15 Many endocrine disruptors have been proven to impair the meiotic process that is mandatory to  
 16 produce healthy gametes. Bisphenol A is emblematic as it impairs meiotic prophase I and causes  
 17 oocyte aneuploidy following *in utero* exposure. However, the mechanisms underlying these  
 18 deleterious effects remain poorly understood. Furthermore, the increasing uses of BPA analogs  
 19 raise concerns for public health. Here, we investigated the effect on oogenesis in mouse of fetal  
 20 exposure to two BPA analogs, Bisphenol A Diglycidyl Ether (BADGE) or Bisphenol AF (BPAF).  
 21 These analogs delay meiosis initiation, increase MLH1 foci *per* cell and induce oocyte aneuploidy.  
 22 We further demonstrate that these defects are accompanied by a deregulation of gene expression  
 23 and aberrant mRNA splicing in fetal premeiotic germ cells. Interestingly, we observed an increase  
 24 in DNA oxidation after exposure to BPA analogs. Specific induction of oxidative DNA damages  
 25 during fetal germ cell differentiation causes similar defects during oogenesis, as observed in 8-  
 26 Oxoguanine DNA Glycosylase (OGG1) deficient mice or after *in utero* exposure to potassium  
 27 bromate (KBrO<sub>3</sub>), an inducer of oxidative DNA damages. Moreover, the supplementation of N-  
 28 acetylcysteine (NAC) with BPA analogs counteracts the bisphenol-induced meiotic effect. Together  
 29 our results position oxidative stress as a central event that negatively impacts the female meiosis  
 30 with major consequences on oocyte quality. This could be a common mechanism of action for so  
 31 called endocrine disruptors pollutants and it could lead to novel strategies for reprotoxic  
 32 compounds.

33 **Keywords:** *development, oogenesis, meiosis, DNA oxidation, bisphenols, endocrine disruptor.*

## 34 Introduction

35 In females, aneuploidy (aberrant number of chromosomes) is an important cause of adverse  
 36 reproductive outcomes such as miscarriages and congenital abnormalities. Aneuploid eggs can be  
 37 induced by numerous lifestyle factors (age, obesity, environmental pollutants...) (Nagaoka et al.,  
 38 2012) and can derive from alterations occurring during meiotic prophase I in fetal life. Indeed,  
 39 proper chromosome segregation at adulthood requires organized reciprocal DNA exchanges  
 40 between homologous chromosomes (crossover) occurring during prophase I as a result of the  
 41 repair of meiotic double strand break (DSB) by homologous recombination (Patricia A. Hunt &  
 42 Hassold, 2008; Ottolini et al., 2015; S. Wang et al., 2017). Crossover regulation depends on a  
 43 correct implementation of the meiotic program in primordial germ cells (PGCs) initiated after their  
 44 migration into the gonad. At this stage, pluripotent and proliferative PGCs acquire the competence  
 45 to initiate meiosis through the expression of Deleted In Azoospermia-like (*Dazl*) (Nicholls et al.,  
 46 2019). Depending on the somatic environment and under the control of meiotic orchestrators such  
 47 as *Stra8* that direct the switch from mitosis to meiosis, female PGCs initiate prophase I at 13.5 day  
 48 post-conception (dpc) (Bailey et al., 2017; Hargan-Calvopina et al., 2016a; Ishiguro et al., 2020; Le  
 49 Bouffant et al., 2010; Spiller & Bowles, 2019; Trautmann et al., 2008). Alterations that occur during  
 50 the establishment of the meiotic program lead to meiotic defects in prophase I that can hamper  
 51 future fertility (Bailey et al., 2017; Hargan-Calvopina et al., 2016a; Ishiguro et al., 2020; Nicholls et  
 52 al., 2019). It is well known that implementation and progression of prophase I are extremely  
 53 sensitive to environmental factors such as toxicants and endocrine disrupting chemicals. Among  
 54 those, bisphenol A (BPA) is the first and the most studied environmental compound known to alter  
 55 meiosis and folliculogenesis in females in numerous mammalian and non-mammalian organisms  
 56 (Brieno-Enriquez et al., 2012; Briño-Enríquez et al., 2011; P. A. Hunt et al., 2012; Lawson et al.,  
 57 2011; Susiarjo et al., 2007; W. Wang et al., 2014; H.-Q. Zhang et al., 2012; T. Zhang et al., 2014).  
 58 In female primates and rodents, fetal exposure to BPA induces alteration of the expression of  
 59 meiotic genes at the time of meiosis onset and during prophase I (Brieno-Enriquez et al., 2012;  
 60 Lawson et al., 2011; H.-Q. Zhang et al., 2012). Moreover, fetal exposure to BPA alters the  
 61 distribution of recombination events signaled by MLH1, a DNA mismatch repair protein required for

62 resolution of double Holliday junctions as crossovers (Ashley et al., 2001; Cheng et al., 2009;  
63 Patricia A. Hunt et al., 2003). This increase observed during pachytene stage is correlated with the  
64 occurrence of aneuploid oocytes at adulthood. The precise action of BPA on meiosis has been  
65 proposed to involve estrogen receptor signaling (Gibert, 2015; Susiarjo et al., 2007; M. Yu et al.,  
66 2018; H.-Q. Zhang et al., 2012). Moreover, several studies suggest that BPA exposure induces  
67 epigenetic alterations in germ cells such as DNA or histone methylation resulting in gene  
68 expression alterations (Chao et al., 2012; Chianese et al., 2017; Kim et al., 2014; T. Wang et al.,  
69 2016; H.-Q. Zhang et al., 2012). Lastly, some studies have shown that post-natal exposure to BPA  
70 increases the amount of reactive oxygen species (ROS) compromising oocyte maturation and  
71 chromosome segregation and inducing DNA damages such as 8-hydroxydeoxyguanosine (8OdG)  
72 (Ganesan & Keating, 2016; M. Zhang et al., 2017; T. Zhang et al., 2018).

73 BPA is a member of the bisphenol family like other structural analogs that are commonly used in  
74 the industry. Due to recent regulations and growing commercialization of BPA-free labeled  
75 products, BPA analogs are increasingly used in the manufacturing of consumer products. Among  
76 those, we choose to focus our study on emerging bisphenols: Bisphenol A Diglycidyl Ether  
77 (BADGE) and Bisphenol AF (BPAF) because very little data exists on their effects on mammalian  
78 germ cells. However, recent studies have shown that, as BPA, BPAF induces the release of ROS  
79 in adult oocytes, delaying *in vitro* maturation (Ding et al., 2017; Jones et al., 2018).

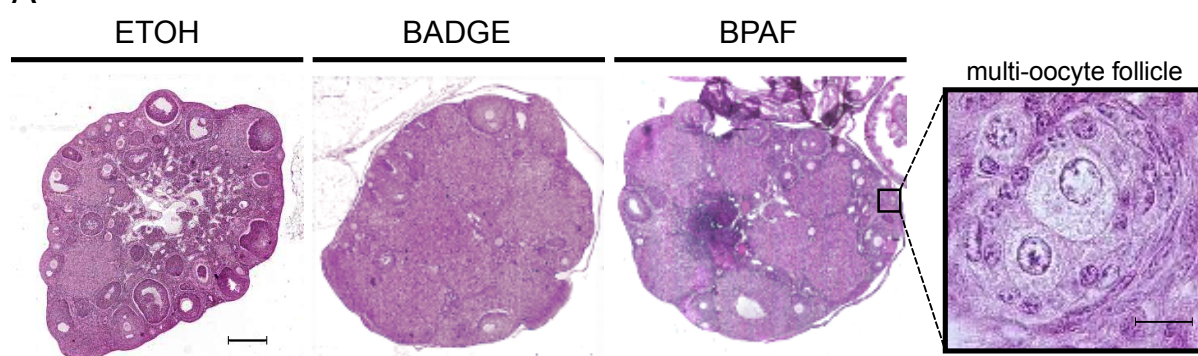
80 The aim of this study was to explore the effects of prenatal exposure of murine oocytes to BADGE  
81 and BPAF and their consequences on fertility at adulthood. We show that exposure of pregnant  
82 mice to the BPA analogs, BADGE and BPAF causes oxidative DNA damage, alterations during  
83 mitosis to meiosis transition and an increase of crossovers number leading to aneuploidy and  
84 oocyte loss. Specific induction of oxidative DNA damages during fetal germ cell differentiation  
85 causes similar defects in prophase I as observed in 8-Oxoguanine DNA Glycosylase (OGG1)  
86 deficient mice and after fetal exposure to potassium bromate. Thus, we unveiled the central role of  
87 oxidative DNA damage in the meiotic response to bisphenols.

## 88 Results

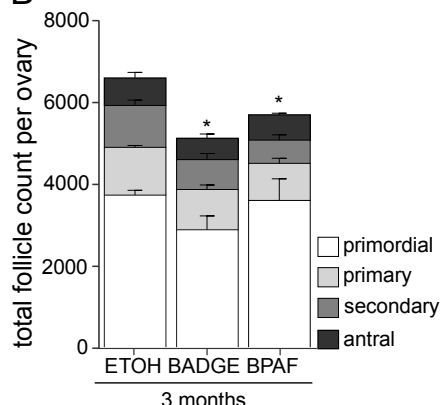
### 89 BADGE or BPAF fetal exposure reproduces BPA defects on folliculogenesis and 90 recombination events.

91 In mammals, fetal exposure to BPA disrupts follicle formation causing multioocyte follicles and  
92 increases the incidence of missegregation after meiosis resumption in post-natal ovaries. To study  
93 the effects of analogs of BPA on oocyte and folliculogenesis at adulthood, we exposed pregnant  
94 mice to 10  $\mu$ M of BADGE or BPAF in drinking water from 10.5 to 18.5 days post-conception.

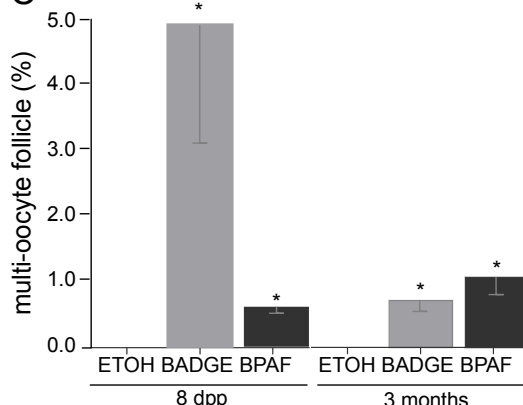
A



B



C



95 **Figure 1: BADGE or BPAF fetal exposures fetal exposure impairs folliculogenesis in post-**  
96 **natal mouse ovaries.** (A) Haematoxylin and eosin staining of ovarian section from 3 months old  
97 mice exposed during fetal life to vehicle (ETOH), BADGE (BADGE) or BPAF (BPAF). Scale bar,  
98 200 $\mu$ m or 10 $\mu$ m for the higher magnification (multi-oocyte follicle). (B) Quantification of total follicle  
99 count in bisphenol-treated or control adult ovaries. Each bar represents the percentage of  
100 primordial, primary, secondary and antral follicles. (C) Percentage of multioocytes follicle in  
101 bisphenols-treated or control post-natal (8 dpp) and adult (3 months) ovaries. Error bars indicate  
102 mean  $\pm$  s.e.m. n=3-5 mice from 3 independent exposures, \* p < 0.05 (Mann-Whitney's test).

103 At 3 months old, the total number of follicles was assayed in treated (BADGE or BPAF) and control  
104 (ethanol [ETOH]) ovaries (Figure 1A-C). A significant decrease of follicular pool was detected in  
105 treated ovaries (Figure 1B). The distribution of follicle classes (primordial to antral follicle) was not  
106 affected by the treatment suggesting that the progression of folliculogenesis was not affected

(Figure 1B). However, we observed abnormal multioocyte follicles in BADGE- and BPAF- treated 3-months ovaries (0 follicle in ETOH group VS  $34 \pm 11$  follicles and  $58 \pm 14$  follicles in BADGE and BPAF groups respectively; Figure 1C). The incidence of multioocyte follicles was even more pronounced at the initiation of the folliculogenesis (*ie* 8 days postpartum) in the BADGE- and BPAF- treated ovaries (0 follicle in ETOH group VS  $647 \pm 262$  follicles and  $75 \pm 11$  follicles in BADGE and BPAF groups respectively; Figure 1C).

As observed with BPA, exposure to bisphenol A analogs induces chromosome missegregation during meiotic divisions. Ploidy in metaphase II oocytes from bisphenols-treated ovaries was assessed by the presence of isolated chromosomes. BADGE or BPAF fetal exposure significantly increases the percentage of aneuploid metaphase II (MII) oocytes (Figure 2A). During prophase I, crossovers and chiasmata distribution in oocyte was also modified after BPAF or BADGE *in utero* exposure. We quantified MLH1 foci in pachytene cells at 18.5 days post-conception (dpc) in bisphenols-treated ovaries. Pachytene stage was identified on the basis of SYCP3 staining patterns and the number of MLH1 foci per bivalent (chromosome pair) was determined. The number of bivalent with three or more MLH1 foci was increased in bisphenols-treated oocytes (Figure 2C). The increase of reciprocal exchanges between homologs was confirmed by the quantification of chiasmata in metaphase I oocytes. In bisphenols-treated oocytes, we observed an increase in bivalent with three or more chiasmata identified according to the shape of the bivalent (Figure 2B). Thus BPAF and BADGE mimic the known hallmarks of BPA during oogenesis like impaired crossovers distribution and aneuploidy.

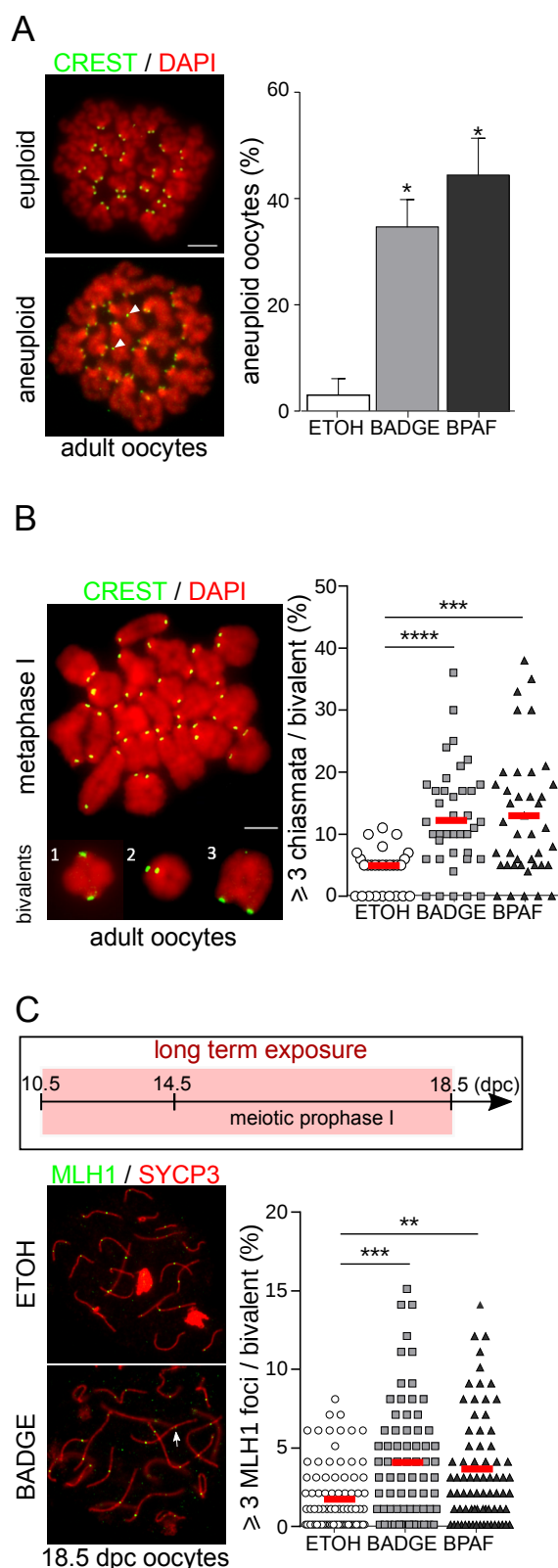


**Figure 2: BADGE or BPAF fetal exposures increase the recombination events and missegregation during meiosis.** (A) Aneuploid MII oocytes in 3 months old mice exposed during fetal life with vehicle (ETOH), BADGE or BPAF were quantified after CREST immunofluorescence staining. Left panel: photomicrographs of representative euploid (20 chromosomes, 40 centromeres) or aneuploid oocytes ( $\neq 20$  chromosomes,  $\neq 40$  centromeres). Arrowhead indicates extra chromatids. Scale bar: 10  $\mu$ m. Right panel: quantification of the percentage of aneuploid MII oocytes.  $n = 28$  (ETOH), 40 (BADGE) and 42 (BPAF) oocytes from 5-12 independent exposures. Mean  $\pm$  s.e.m, \*  $p < 0.05$  (Mann-Whitney's test). (B) The number of chiasmata per bivalent (tetrad) in MI oocytes from 3 months old mice exposed during fetal life with vehicle (ETOH), BADGE or BPAF were determined according to the shape of the bivalent after CREST immunostaining (green). Left panel: representative photomicrograph of MI oocyte that contains tetrads with one (1), two (2), three or more (3) chiasmata. Scale bar: 10  $\mu$ m. Right panel: percentage of bivalent with 3 or more chiasmata.  $n = 33$  (ETOH), 56 (BADGE) and 23 (BPAF) oocytes from 5 independent exposures. Mean (red bar), \*\*\*  $p < 0.001$ , \*\*\*\*  $p < 0.0001$  (Mann-Whitney's test). (C) Ovaries from fetuses exposed to vehicle (ETOH) or bisphenols (BADGE and BPAF) from 10.5 dpc to 18.5 dpc were used for the MLH1 quantification (long exposure). The number of crossovers per synaptonemal complexes (synapsis) in pachytene oocytes from 18.5 dpc fetuses was quantified using MLH1 immunostaining (green). The pachytene stage is determined on the basis of the SYCP3 staining (red). Left panel: Representative photomicrographs of pachytene cells from vehicle (ETOH) and BADGE treated ovaries. White arrow shows a synaptonemal complex with 3 MLH1 foci. Right panel: Percentage of synaptonemal complexes with 3 or more MLH1 foci.  $n = 86$  (ETOH), 78 (BADGE) and 82 (BPAF) oocytes from 12 independent exposures. Mean: red bar, \*\*  $p < 0.01$ ; \*\*\*  $p < 0.001$ .

# **BADGE or BPAF fetal exposures delay meiotic progression and initiation**

At 18.5 dpc, we observed a delay in meiotic progression in bisphenols-treated mice with a decrease in the proportion of diplotene stages in favor to the early and late pachytene stages (Figure 3A).

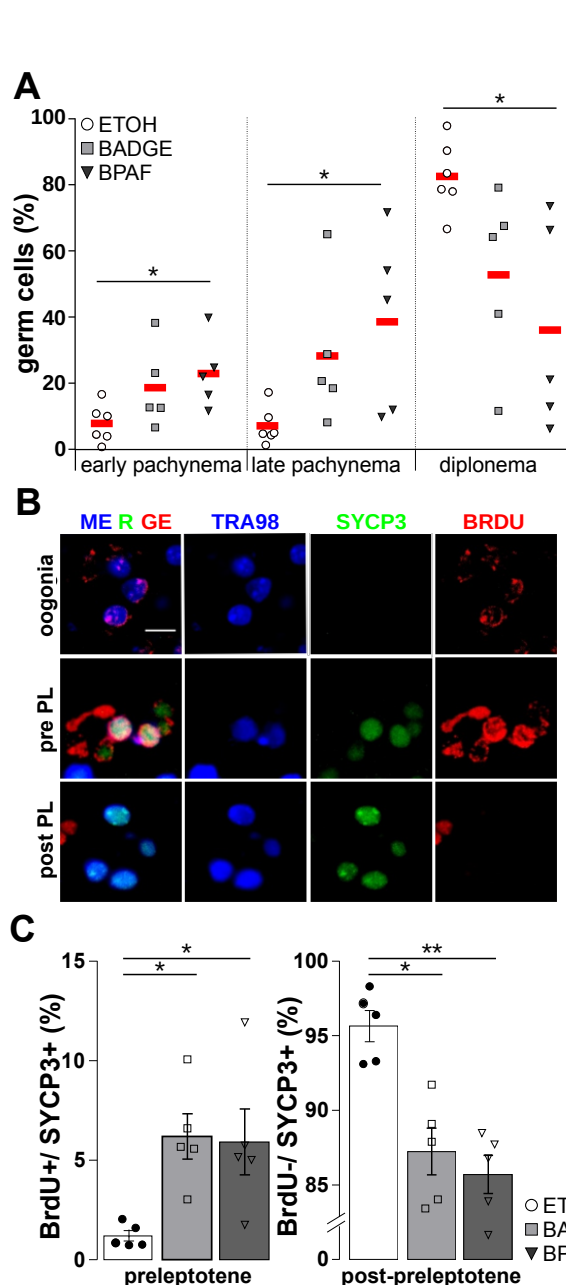
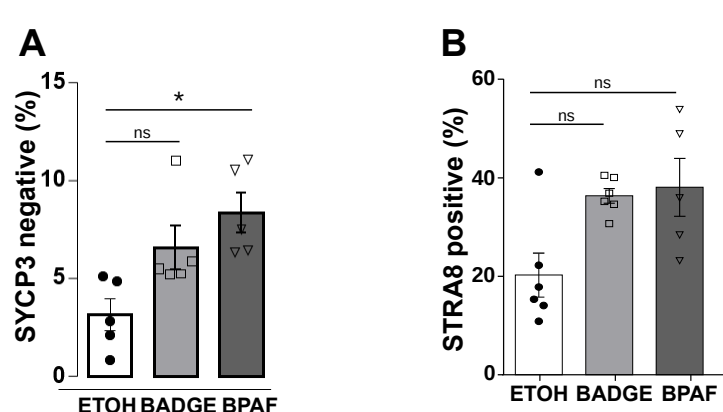


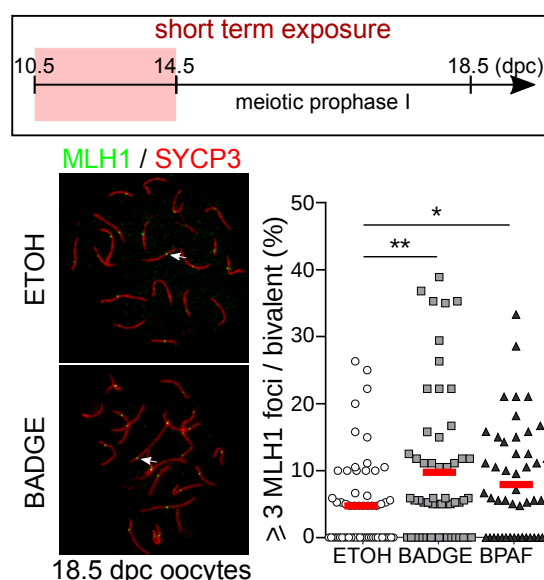
**Figure 3: BADGE or BPAF fetal exposures delay the meiosis initiation and prophase I progression.** (A) Distribution of meiosis prophase I late stages in 18.5 dpc treated (BADGE, BPAF) and control (ETOH) ovaries. Error bars show mean  $\pm$  s.e.m.; mice analysed  $n=3-6$ ; \*  $p < 0.05$  (Mann-Whitney's test). (B-C) prophase I initiation was assayed in 14.5 dpc ovaries after immunostaining of SYCP3 (meiosis), BrdU (mitosis and meiosis S phase) and TRA98 (germ cell marker). (B) Representative photomicrographs of SYCP3 (green), BrdU (red) and TRA98 (blue) immunostaining. Scale bar 5  $\mu$ m. Pre PL = pre-leptotene; post PL = post-leptotene. Error bars show mean  $\pm$  s.e.m.  $n=5$  mice from independent exposures; \*  $p \leq 0.05$ ; \*\*  $p \leq 0.01$  (Mann-Whitney's test). (C) Graphs showing the percentage of preleptotene (BrdU and SYCP3 positive) and meiotic (BrdU negative, SYCP3 positive) oocytes. Error bars show mean  $\pm$  s.e.m.  $n=5$  mice from independent exposures; \*  $p < 0.05$ ; \*\*  $p < 0.01$  (Mann-Whitney's test).

This defect in meiosis progression could be the consequence of a delay in meiosis initiation. Immunostainings for BrdU, SYCP3 and a germ cells marker (TRA98), were used to identify three germinal populations 14.5 dpc ovaries: oogonia, the female PGCs (SYCP3-negative cells), premeiotic cells in S-phase also called pre-leptonema (BrdU-positive/SYCP3-positive) and oocytes (BrdU-negative/SYCP3-positive; Figure 3B-C). In untreated 14.5 dpc ovaries almost all germ cells had initiated meiosis (over 96% are SYCP3+) and very few oogonia and preleptotene cells were still present. In bisphenols-treated mice, we observed a significant increase in mitotic PGCs (Supplementary Figure 1A) and pre-leptonema while oocyte number was reduced (Figure 3C).



**Supplementary Figure 1 :** (A) Percentage of oocytes (SYCP3-/TRA98 positive). Error bars show mean  $\pm$  s.e.m.  $n=5$  mice from independent exposures; \*  $p < 0.05$  (Mann-Whitney's test). (B) Percentage of germ cells expressing STRA8 in 14.5 dpc female gonads.  $n=5$  mice from independent exposures;  $p=0.08$  (BADGE),  $p=0.07$  (BPAF) (Mann-Whitney's test).

In addition, we observed an increasing trend for STRA8 positive germ cells in 14.5 dpc female gonads (20%  $\pm$  4 in ETOH group VS 36%  $\pm$  1  $p=0.08$  and 39%  $\pm$  6,  $p=0.07$  in BADGE and BPAF groups respectively, Supplementary Figure 1B). The presence of STRA8 correlated with the initiation of the meiotic program and declines rapidly just after the initiation in prophase I. The observed increase confirmed the bisphenols-induced delay of meiotic initiation. A defect of crossover distribution could be the consequence of a delay and/or an alteration of meiosis initiation. To confirm this hypothesis, we performed exposure to bisphenols until meiosis initiation (short term exposure).



**Supplementary Figure 2:** Ovaries from fetuses exposed to vehicle (ETOH) or bisphenols (BADGE and BPAF) from 10.5 dpc to 14.5 dpc were used for the MLH1 quantification (short exposure). Left panel: Representative photomicrographs of pachytene cells from vehicle (ETOH) and BADGE treated ovaries. White arrow shows a synaptonemal complex with 3 MLH1 foci. Right panel: Percentage of synaptonemal complexes with 3 or more MLH1 foci.  $n=62$  (ETOH), 55 (BADGE) and 55 (BPAF) oocytes from 3 independent exposures. Mean (red bar), \*  $p < 0.05$ , \*\*  $p < 0.01$  (Mann-Whitney's test).

Fetuses were exposed from 10.5 to 14.5 dpc (Supplementary Figure 2, upper panel) and the MLH1 foci was quantified at 18.5 dpc. As observed for bisphenols exposures during meiosis progression (long-term exposure), the number of MLH1 foci was significantly increased after bisphenols exposure (Supplementary Figure 2). This suggests that changes in crossovers distribution were

probably due to alterations occurring before or during mitosis to meiosis transition in germ cells (GCs).

## **BADGE or BPAF fetal exposures alter gene expression and mRNA splicing in germ cells**

In order to understand the bases of bisphenols-induced alterations in PGCs during acquisition of meiotic competence and initiation of the meiotic program, we performed transcriptomic analyses on 11.5 dpc (during acquisition of the meiotic competence) and 13.5 dpc (during meiosis initiation) germ cells. We sorted PGCs by Magnetic Activated Cell Sorting (MACS) using the cell surface protein stage-specific embryonic antigen 1 (SSEA-1). Gene expression analysis was conducted using murine Affymetrix GeneChip Gene 2.0 TS (11.5 dpc) and Clariom™ D (13.5 dpc) microarrays. At 11.5 dpc, we identified 1817 and 733 differentially expressed genes (DEGs) in BADGE and BPAF treated germ cells respectively (compared to vehicle treated PGCs with a  $|\text{Log}_2 \text{Fold-Change}| \geq 0.5$  and  $p < 0.05$ ) (Figure 4). DEGs were mostly downregulated (56 to 65 % of DEGs; Figure 4A). At 13.5 dpc when the program of meiosis is initiated, we identified 886 and 1376 DEGs in BADGE and BPAF treated germ cells respectively (Figure 4A). Contrary to what it is observed at 11.5 dpc, two third of the DEGs were upregulated in 13.5 dpc bisphenols-treated germ cells (Figure 4A). Using EnrichGO function from ClusterProfiler package to identify enrichment of gene ontologies, we observed that DEGs at 11.5 dpc as well as 13.5 dpc were mostly related to meiosis, stem cell differentiation and regulation of stem cell signaling pathway such as Wnt pathway (Figure 4B and Supplementary Figure 3). Meiosis-associated DEGs such as *Stag3*, *Sycp1&3*, *Hormad1&2*, *Spo11*, *Spata22*, *Meiob*, *Dmc1* or *Brca2* were strongly enriched in genes associated to synapsis and DNA recombination processes (Figure 4A-C, Supplementary Table 1). Surprisingly, genes linked to meiosis and stem cell differentiation showed opposite transcriptional response at 11.5 dpc and 13.5 dpc (Supplementary Figure 3 and Figure 4C). Stemness genes tend to be up-regulated at 11.5 dpc and mostly down-regulated at 13.5 dpc and meiotic genes were preferentially down-regulated at 11.5 dpc and up-regulated at 13.5 dpc (Figure 4C).

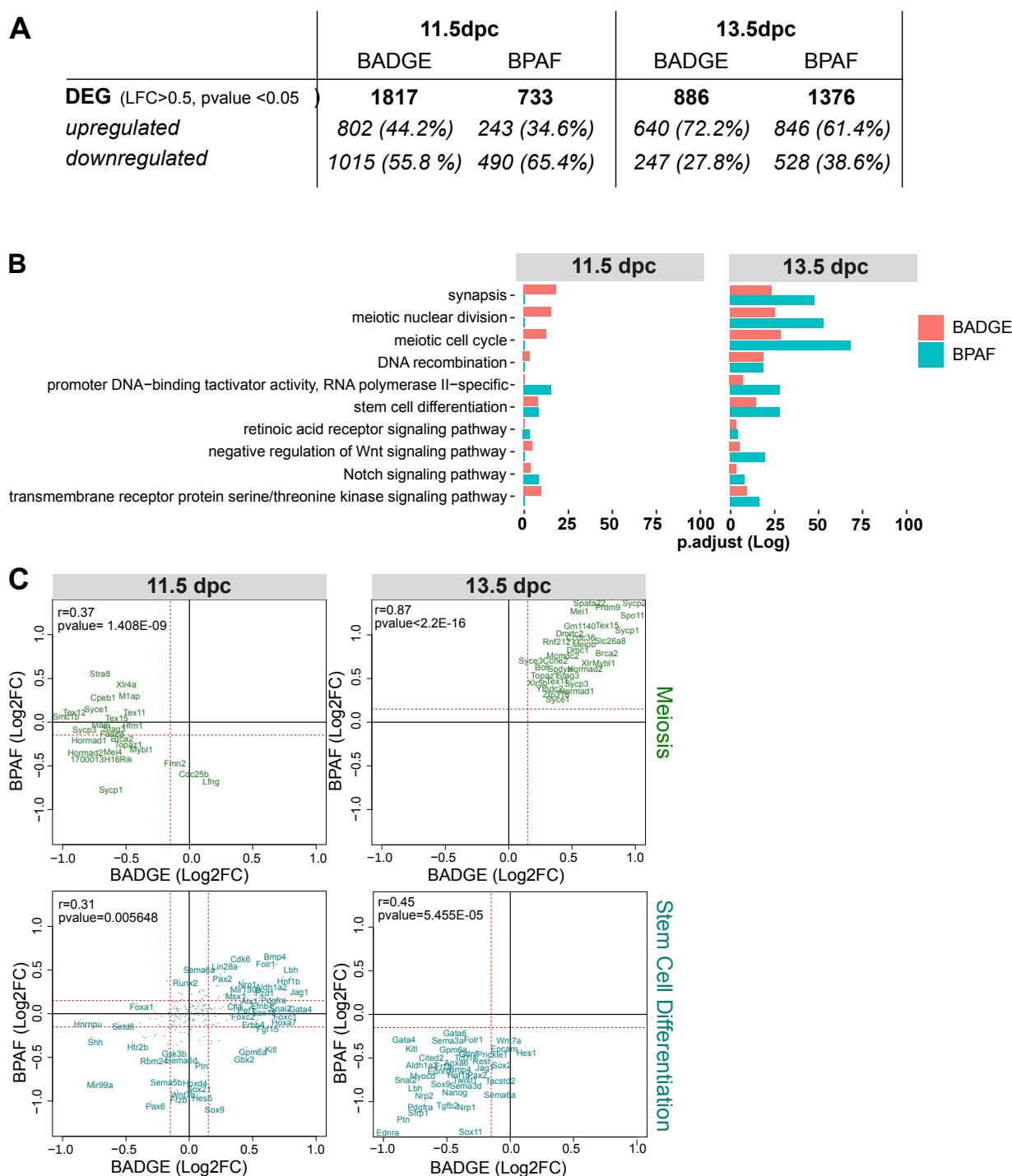


**Figure 4: BADGE or BPAF fetal exposures induce transcriptional alteration before meiosis initiation.** SSEA1 positive germ cells from 11.5 or 13.5 dpc ovaries treated by vehicle (ETOH) or bisphenols (BADGE and BPAF) were used for transcriptomic analyses. Differentially expressed genes (DEGs) between bisphenols and control condition (BPAF vs ETOH or BADGE vs ETOH) were filtered according to the log fold change ( $abs[Log2FC] \geq 0.5$ ) and the significance ( $p < 0.05$ ). Three pools of cells each of them from 10-15 fetuses were analyzed. (A) The table represents the number (and percentage) of DEGs after BADGE or BPAF exposure in 11.5 or 13.5 dpc germ cells. (B) Gene Ontology enrichment associated to meiosis and stem cell differentiation among DEGs. (C) Correlation analysis between BADGE and BPAF condition of the differential expression (Log2FC) of genes associated to meiosis or stem cell differentiation.  $r$  = Pearson's correlation coefficient (Pearson's test).



283 **Supplementary Figure 3.** Enrichment of Gene Ontology (biological process, molecular function  
 284 and cellular component) of DEGs after bisphenols exposure in 11.5 and 13.5 dpc. Ontologies  
 285 associated to down-regulated genes is presented as negative values of *p*values.

286 Interestingly, we observed a significant correlation between BPAF and BADGE of the differential  
 287 expression of genes associated to meiosis after bisphenols exposure ( $r=0.37$ ,  $pvalue < 0.0001$ ,  
 288 11.5dpc and  $r=0.87$ ,  $pvalue < 0.0001$ , 13.5 dpc) and stem cell ( $r=0.32$ ,  $p<0.0001$ , 11.5 dpc and  
 289  $r=0.45$ ,  $p < 0.0001$ , 13.5 dpc) at 11.5 dpc and 13.5 dpc (Figure 4C). These positive correlations  
 290 demonstrate a common transcriptional signature between BPAF and BADGE exposure and  
 291 suggest similar mechanisms of action for both bisphenols. Interestingly, as observed in the  
 292 chromosomes 3, 4, 7, 10, 14, and 17, genome mapping of DEGs (up- and down-regulated)  
 293 showed a concentration of genes on specific genome locations that were differentially expressed  
 294 after BADGE and BPAF exposure at 11.5 dpc as well as 13.5 dpc (Supplementary Figure 5).

295 A regulated alternative splicing program has been reported during meiosis initiation in male and in  
 296 female germ cells (Naro et al., 2017; J. Wang et al., 2019). The exact role of this program is  
 297 unclear but is thought to be required for stabilization of meiotic transcripts during prophase I of  
 298 meiosis (Liu et al., 2017; J. Wang et al., 2019). As observed in adult testis, modulation of this  
 299 program results in spermatogenesis defects, highlighting the essential role of the RNA splicing  
 300 during meiosis (Hannigan et al., 2017; Liu et al., 2017). For this reason, we studied the impact of  
 301 bisphenols exposure on RNA splicing events during meiosis initiation. We took advantage of the  
 302 Clariom™ D that allows the detection of most RNA splicing events by covering independently  
 303 exons and exons junctions of all transcripts. After bisphenols exposure, 3543 (BADGE) and 2678  
 304 (BPAF) coding or non-coding genes showed one or more alternative RNA splicing events  
 305 compared to the control condition (Figure 5A-C). Differentially spliced genes were strongly  
 306 associated with chromosome segregation, meiotic cell cycle and DNA repair and recombination  
 307 (Figure 5A). Half of them were identical in BADGE and BPAF -treated germ cells including genes  
 308 such as *Smc4*, *Sun1*, *Mcmhc2*, *Dazl*, *Rad51*, *Mlh1*, *Dmc1*, *Sycp2* (Table1 and Supplementary  
 309 Table 2). Different modes of alternative splicing including skipped exons, alternative 5' splice sites,  
 310 alternative 3' splice sites, and retained intron are described in metazoans. TAC software classifies  
 311 some of these events in function of the coverage of the probes sets of the array. Bisphenols-  
 312 treated germ cells showed an enrichment of transcripts with skipped exon features in all genes  
 313 including meiotic specific genes (Figure 5B, Table 2).

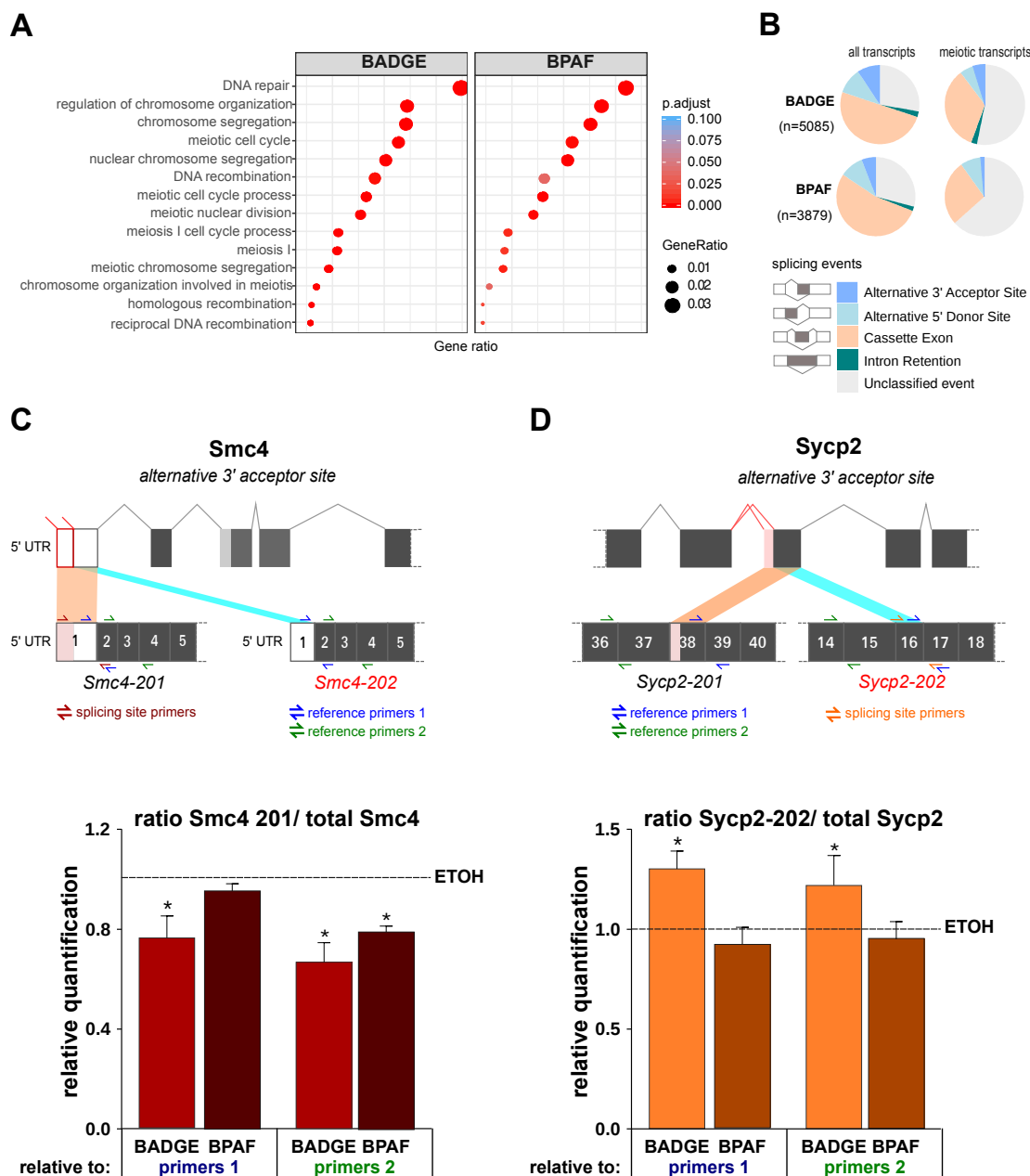


**Figure 5: BADGE or BPAF fetal exposures induce RNA splicing alterations in premeiotic germ cells.** Splicing events were determined in 13.5 dpc germ cells using the high resolution microarray. Using TAC software, differentially spliced genes (BPAF vs ETOH and BADGE vs ETOH) were filtered according to the exon splicing index ( $abs[\text{exon splicing index}] \geq 1$ ) and the exon  $p$ value ( $p < 0.05$ ).  $n = 3$  pools of cells from 10-15 fetuses each. (A) dot plot showing enrichment on ontology associated to meiosis of differentially spliced genes. (B) distribution of splicing events in all genes and specifically meiotic genes. Modes of alternative splicing including skipped exons, alternative 5' splice sites, alternative 3' splice sites, and retained intron. Unclassified events correspond to events that cannot be included in any of the standard categories. (C) and (D) Quantification of the relative incidence of *Smc4* (C) and *Sycp2* (D) splice variants (Ensembl variants:) in bisphenols-treated germ cells.  $n = 3$  independent exposures. Upper panel: Representation of splicing sites leading to different splice variants (*Smc4*-201, *Smc4*-202, *Sycp2*-201 and *Sycp2*-202, Ensembl name). Lower panel: relative quantification of expression of *Smc4*-201 or *Sycp2*-202 to total *Smc4* transcripts and *Sycp2* transcripts respectively in bisphenols treated germ cells in comparison to ETOH-treated germ cells. \*  $p < 0.05$  (Mann-Whitney's test).

329 **Table 1: List of common genes between BADGE and BPAF conditions showing an**  
 330 **alternative splicing relative to control germ cell.**

Go term	Differentially Spliced genes count (adj <i>pvalue</i> )	Common genes between bisphenols	
		%	common genes
Chromosome Segregation (GO:0007059)	105 (BADGE ; <i>pvalue</i> 9 x10 <sup>-8</sup> ) 85 (BPAF; <i>pvalue</i> 2 x10 <sup>-6</sup> )	46% (BADGE) 56% (BPAF)	<i>Smc4, Espl1, Mms19, Srp1, Cit, Ccne1, Psr1, Bub1b, Pttg1, Kif4, Mlh1, Dync1h1, Zw10, Zwint, Cep63, Hecw2, Spag5, Pogz, Pum1, Mcmdc2, Top2b, Bub1, Setdb2, Anapc1, Atm, Pibf1, Mst1, Mau2, Cdc20, Ndc1, Fancd2, Usp9x, Top3b, Tpr, Ago4, Ncapd3, Sun1, Cenph, Nipbl, Ddx11, Hira, Csnk2a1, Lrrk1, Smc1b, Ino80, Dmc1, Hfm1</i>
DNA repair (GO:0006281)	151 (BADGE; <i>pvalue</i> : 5 x10 <sup>-10</sup> ) 108 (BPAF; <i>pvalue</i> : 7 x10 <sup>-6</sup> )	44 % (BADGE) 61 % (BPAF)	<i>Nhej1, Nabp1, Pold2, Gins4, Wrm, Uchl5, Smc4, Hdac9, Npas2, Usp47, Mms19, Prkdc, Pms2, Fanci, Pif1, Upf1, Pttg1, Rad51, Mlh1, Cdc45, Kdm2a, Usp3, Otub1, Abl1, Dclre1a, Shprh, Parp9, Cep164, Neil1, Marf1, Rbm17, Mcmdc2, Npm1, Top2b, Taok3, Ticrr, Cdc5l, Supt16, Xpc, Atm, Rad52, Uimc1, Poli, Ube2t, Taok1, Rbbp8, Fancd2, Setx, Sprtn, Ercc6l2, Gtf2h1, Nipb, Atr, Alkbh1, Ddx11, Usp28, Eya1, Rtel1, Rif1, Rev1, Cdc7, Ino80, Dmc1, Huwe1, Helq</i>
Nuclear Chromosome Segregation (GO:0098813)	88 (BADGE; <i>pvalue</i> : 3 x10 <sup>-07</sup> ) 70 (BPAF; <i>pvalue</i> : 12 x10 <sup>-05</sup> )	45 % (BADGE) 57 % (BPAF)	<i>Smc4, Espl1, Cit, Ccne1, Psr1, Bub1b, Pttg1, Kif4, Mlh1, Dync1h1, Zw10, Zwint, Cep63, Hecw2, Spag5, Pogz, Mcmdc2, Top2b, Bub1, Anapc1, Atm, Pibf1, Mst1, Mau2, Cdc20, Ndc1, ancd2, Tpr, Ago4, Ncapd3, Sun1, Nipbl, Ddx11, Hira, Lrrk1, Smc1b, Ino80, Dmc1, Hfm1</i>
DNA Recombination (GO:0006310)	79 (BADGE, <i>pvalue</i> < 0.001) 5 (BPAF, <i>pvalue</i> : 0.04)	40 % (BADGE) 58 % (BPAF)	<i>Cntd1, Nabp1, Gins4, Ubr2, Wrm, Uchl5, Rag1, Mms19, Prkdc, Pms2, Pif1, Rad51, Mlh1, Cdc45, Cep63, Thoc1, Mcmdc2, Top2b, Atm, Rad52, Rbbp8, Setx, Psmc3ip, Nipbl, Rtel1, Rif1, Cdc7, Ino80, Dmc1, Hfm1, Gm960, Helq</i>
Meiotic Cell Cycle process (GO:0051321)	99 (BADGE; <i>pvalue</i> : 2 x10 <sup>-06</sup> ) 73 (BPAF; <i>pvalue</i> <0.001)	11 % (BADGE) 15% (BPAF)	<i>Tdrd9, Cntd1, Topaz1, Ubr2, Smc4, Espl1, Ccne1, Bub1b, Pttg1, Rad51, Mlh1, Marf1, Cep63, Plcb1, Nsun2, Mcmdc2, Top2b, Bub1, Atm, Cdc20, Ndc1, Fancd2, Psmc3ip, Ago4, Ncapd3, Sun1, Lrrk1, Aspm, Dmc1, Hfm1, Gm960, Sycp2</i>

331 **Table 2: Splicing event estimation by TAC software in bisphenols treated germ cells.** EEJ:  
 332 one exon-exon junction was covered by probes, E: one exon was covered by probes. Only PSRs  
 333 have assigned « Event Estimation Name ». Embedded text: common significative splicing events  
 334 between BADGE and BPAF.

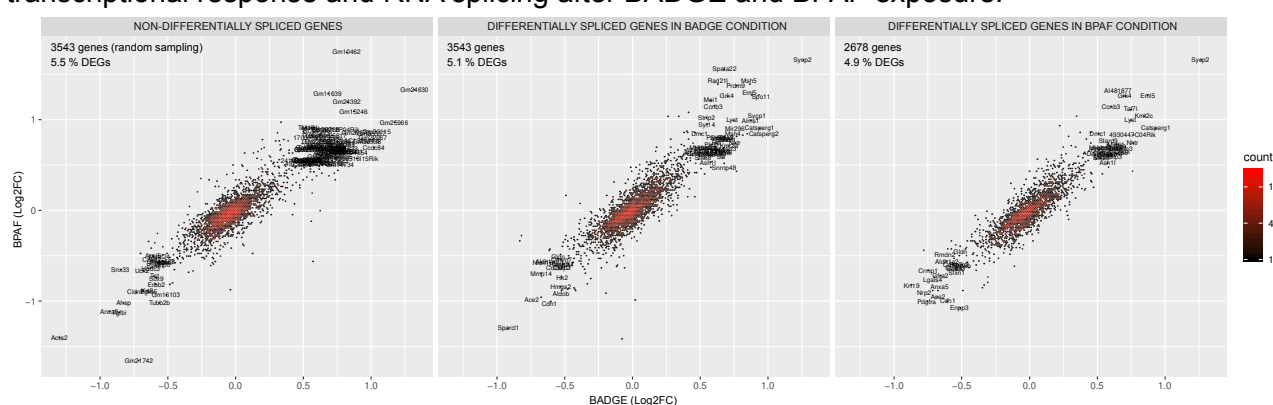
Gene Symbol	Probes			Splicing event estimation name	Splicing event ( $p < 0.01$ )		<i>pvalue</i>
	target	location	Isoform name		BADGE	BPAF	
<i>Ago4</i>	EEJ	Exons 11-12	Ago4-201	-	ns		0.0028
	EEJ	Exons 9-10	Ago4-201	-	0.0093		ns
<i>Aspm</i>	EEJ	Exons 1-2	Aspm-201	-	0.0007		ns
	E	Exon 18	Aspm-201	ND	ns		0.0044
<i>Atm</i>	EEJ	<b>Exons 56-57</b>	<b>Atm-201</b>	-	<b>0.0061</b>		<b>0.0093</b>
	EEJ	Exons 52-53	Atm-201	-	ns		0.0061
	EEJ	Exons 47-48	Atm-201	-	0.0039		ns
	EEJ	<b>Exons 49-50</b>	<b>Atm-201</b>	-	<b>0.002</b>		<b>0.0017</b>
	E	Exon 29	Atm-201	Cassette Exon	0.01		ns
<i>Bub1b</i>	EEJ	<b>Exons 9-10</b>	<b>Bub1-201</b>	-	<b>0.0002</b>		<b>0.0044</b>
	E	Exon 1	Bub1-203	Alt 3' Acceptor Site	ns		0.0064
<i>Ccne1</i>	EEJ	Exons 6-7	Ccne-201	-	ns		0.0026
	E	Exon 1	Ccne-201	Cassette Exon	0.0035		ns
<i>Cdc7</i>	EEJ	<b>Exons 6-8</b>	<b>Cdc7-201</b>	-	<b>0.0044</b>		<b>0.0366</b>
<i>Cdc20</i>	EEJ	Exons 6-7	Cdc20-201	-	0.0041		ns
	E	Exon 1	Cdc20-201	Cassette Exon	ns		0.004
<i>Cdc45</i>	EEJ	Exons 19-20	Cdc45-201	-	ns		0.0089
	EEJ	Exons 11-12	Cdc45-201	-	0.009		ns
	EEJ	Exons 1-2	Cdc45-201	-	0.0094		ns
<i>Cep63</i>	E	<b>Exon 7</b>	<b>Cep63-201</b>	<b>Cassette Exon</b>	<b>0.0024</b>		<b>0.0047</b>
<i>Cntd1</i>	E	Exon 1 (-5')	Cntd1-201	Cassette Exon	ns		0.007
	E	Exon 1 (-3')	Cntd1-201	Cassette Exon	ns		0.0074
	E	Exon 3	Cntd1-203	Cassette Exon	0.0012		ns
<i>Dmc1</i>	EEJ	<b>Exons 9-10</b>	<b>Dmc1-201</b>	-	<b>0.0004</b>		<b>0.0069</b>
	EEJ	Exons 7-8	Dmc1-201	-	0.0013		ns
<i>Espl1</i>	EEJ	<b>Exons 1-2</b>	<b>Espl1-201</b>	-	<b>0.003</b>		<b>0.0039</b>
<i>Fancd2</i>	EEJ	<b>Exons 22-23</b>	<b>Fancd2-201</b>	-	<b>0.0019</b>		<b>0.0088</b>
	EEJ	Exons 31-32	Fancd2-201	-	0.0096		ns
<i>Gins4</i>	EEJ	Exons 2-3	Gins4-201	-	0.0061		ns
	E	Exon 8	Gins4-201	Alt 5' Donor Site	ns		0.0045
<i>Gm960 (Top6bl)</i>	EEJ	Exons 3-4	Gm960-201	-	ns		0.0039
	E	Exon 12	Gm960-202	Cassette Exon	0.0033		ns
	E	Exon 11	Gm960-202	Cassette Exon	0.0076		ns
<i>Helq</i>	EEJ	<b>Exons 16-17</b>	<b>Helq-201</b>	-	<b>0.0000157</b>		<b>0.0038</b>
	EEJ	Exons 12-13	Helq-201	-	0.0088		ns
<i>Hfm1</i>	EEJ	Exons 7-8	Hfm1-201	-	ns		0.0076
	E	Exon 22	Hfm1-201	Cassette Exon	0.0031		ns
	E	Exon 21	Hfm1-201	Cassette Exon	0.0087		ns
	E	Exon 4	Hfm1-204	Cassette Exon	0.0005		ns

<b>Ino80e</b>	<b>EEJ</b>	<b>Exons 2-3</b>	<b>Ino80e-203</b>	-	<b>0.0007</b>	<b>0.0034</b>
<b>Lrrk1</b>	<b>E</b>	<b>Exon 28</b>	<b>Lrrk1-201</b>	<b>Cassette Exon</b>	<b>0.0077</b>	<b>0.0042</b>
<b>Marf1</b>	EEJ	Exons 24-25	Marf1-201	-	ns	0.0084
	EEJ	<b>Exons 9-10</b>	<b>Marf1-201</b>	-	<b>0.0023</b>	<b>0.0069</b>
<b>Mcm2dc2</b>	E	Exon 10	Mcm2dc2-201	-	ns	0.0096
	E	Exon 14	Mcm2dc2-203	Cassette Exon	0.0047	n
	E	Exon 16	Mcm2dc2-204	Alt 5' Donor Site	0.0018	ns
<b>Mlh1</b>	EEJ	Exons 15-17	Mlh1-201	-	ns	0.0091
	E	Exon 18	Mlh1-206	ND	0.0056	ns
	E	Exon 18	Mlh1-201	ND	0.0035	ns
<b>Mms19</b>	<b>EEJ</b>	<b>Exons 4-6</b>	<b>Mms19-201</b>	-	<b>0.0008</b>	<b>0.007</b>
	E	Exon 28	Mms19-201	Cassette Exon	ns	0.0022
	<b>E</b>	<b>Intron 6</b>	<b>Mms19-201</b>	<b>Intron Retention</b>	<b>0.0066</b>	<b>0.0021</b>
	E	Exon 6	Mms19-201	Cassette Exon	0.0094	ns
<b>Nabp1</b>	EEJ	Exons 5-6	Nabp1-204	-	0.0088	ns
	E	Exon 1	Nabp1-208	Alt 5' Donor Site	0.004	ns
	E	Exon 6	Nabp1-201	ND	ns	0.0056
<b>Ncapd3</b>	EEJ	Exons 29-30	Ncapd3-201	-	ns	0.0065
	E	Exon 4	Ncapd3-201	Cassette Exon	0.0069	ns
	E	Exon 26	Ncapd3-201	Cassette Exon	0.0047	ns
	E	Exon 29	Ncapd3-201	Cassette Exon	0.0041	ns
<b>Ndc1</b>	<b>EEJ</b>	<b>Exons 1-2</b>	<b>Ndc1-205</b>	-	<b>0.0018</b>	<b>0.0032</b>
<b>Nipbl</b>	EEJ	Exons 25-26	Nipbl-201	-	0.001	ns
	E	Exon 28	Nipbl-201	Cassette Exon	ns	0.004
	E	Exon 16	Nipbl-201	Cassette Exon	ns	0.0055
<b>Nsun2</b>	EEJ	Exons 7-8	Nsun2-201	-	0.002	ns
	EEJ	Exons1-2	Nsun2-203	-	ns	0.0045
<b>Plcb1</b>	<b>E</b>	<b>Exon 32</b>	<b>Plcb1-201</b>	<b>Cassette Exon</b>	<b>0.0017</b>	<b>0.0079</b>
<b>Prkdc</b>	<b>EEJ</b>	<b>Exons 52-53</b>	<b>Prkdc-201</b>	-	<b>0.0039</b>	<b>0.0079</b>
<b>Psmc3ip</b>	<b>EEJ</b>	<b>Exons 2-3</b>	<b>Psmc3ip-201</b>	-	<b>0.0025</b>	<b>0.0059</b>
<b>Pttg1</b>	<b>E</b>	<b>Exon 1</b>	<b>Pttg1-201</b>	<b>Alt 5' Donor Site</b>	<b>0.0026</b>	<b>0.0026</b>
<b>Rad51</b>	EEJ	Exons 1-2	Rad51-201	-	0.0064	ns
	EEJ	Exons 7-8	<b>Rad51-201</b>	-	<b>0.0023</b>	<b>0.0012</b>
<b>Rag1</b>	E	Exon 6	Rag1-201	Cassette Exon	0.01	ns
	E	Exon 1	Rag1-207	Cassette Exon	ns	0.0085
<b>Rif1</b>	<b>EEJ</b>	<b>Exons 24-25</b>	<b>Rif1-201</b>	-	<b>0.003</b>	<b>0.0058</b>
	E	Exon 5	Rif1-201	Cassette Exon	0.0068	ns
	E	Exon 18	Rif1-201	Cassette Exon	ns	0.0083
	E	Exon 22	Rif1-201	ND	ns	0.0027
<b>Rbbp8</b>	<b>EEJ</b>	<b>Exons 15-16</b>	<b>Rbbp8-201</b>	-	<b>0.000084</b> <b>1</b>	<b>0.0002</b>
<b>Rtel1</b>	EEJ	Exons 6-7	Rtel1-201	-	ns	0.0025
	E	Exon 18	Rtel1-201	Cassette Exon	0.005	ns
<b>Setx</b>	EEJ	Exons 17-18	Setx-201	-	0.0082	ns
	<b>E</b>	<b>Exon 4</b>	<b>Setx-201</b>	<b>Cassette Exon</b>	<b>0.0067</b>	<b>0.0041</b>

> <i>Smc4</i>	EEJ	Exons 9-10	Smc4-201	-	ns	0.0072
	EEJ	Exons 19-20	Smc4-201	-	ns	0.0061
	> E	<b>Exon 1</b>	<b>Smc4-201</b>	<b>Alt 3' Acceptor Site</b>	<b>0.0039</b>	<b>0.0024</b>
	<b>E</b>	<b>Exon 8</b>	<b>Smc4-201</b>	<b>Alt 5' Donor Site</b>	<b>0.0034</b>	<b>0.0049</b>
> <i>Sycp2</i>	EEJ	Exons 36-37	Sycp2-201	-	0.0022	ns
	> E	Exon 38	Sycp2-201	Alt 3' Acceptor Site	0.0027	ns
	<b>E</b>	<b>Exon 36</b>	<b>Sycp-201</b>	<b>Cassette Exon</b>	<b>0.0000384</b>	<b>0.0003</b>
<i>Sun1</i>	EEJ	Exons 8-10	Sun1-201	-	0.0094	ns
	EEJ	Exons 13-14	Sun1-201	-	0.0089	ns
	EEJ	Exons 2-3	Sun1-218	-	0.0063	ns
	EEJ	Exons 6-8	Sun1-201	-	0.0055	ns
	<b>E</b>	<b>Exon 1</b>	<b>Sun1-215</b>	<b>ND</b>	<b>0.0003</b>	<b>0.01</b>
	E	Exon 4	Sun1-201	Alt 3' Acceptor Site	0.0094	ns
	E	Exon 15	Sun1-201	Cassette Exon	0.0076	ns
	<b>E</b>	<b>Exon 17</b>	<b>Sun1-201</b>	<b>Cassette Exon</b>	<b>0.0007</b>	<b>0.01</b>
	E	Exon 18	Sun1-201	Alt 3' Acceptor Site	0.0081	ns
	E	Exon 23	Sun1-201	Alt 5' Donor Site	ns	0.01
<i>Tdrd9</i>	E	Exon 5	Tdrd9-201	Cassette Exon	ns	0.0026
	E	Exon 6	Tdrd9-201	Cassette Exon	ns	0.0077
	E	Exon 24	Tdrd9-201	Cassette Exon	0.005	ns
<i>Thoc1</i>	EEJ	Exons 3-4	Thoc1-201	-	ns	0.01
	E	Exon 7	Thoc1-201	Cassette Exon	0.0054	ns
<i>Top2b</i>	EEJ	Exons 6-7	Top2b-201	-	ns	0.009
	EEJ	Exons 22-23	Top2b-201	-	0.0096	ns
	EEJ	Exons 25-26	Top2b-201	-	0.008	ns
<i>Topaz</i>	EEJ	Exons 4-5	Topaz1-201	-	0.0038	ns
	EEJ	Exons 9-10	Topaz1-201	-	ns	0.0047
	E	Exon 10	Topaz1-201	Cassette Exon	0.0014	ns
<i>Ubr2</i>	E	Exon 1	Ubr-201	ND	0.007	ns
	EEJ	Exons 44-45	Ubr-201	-	ns	0.005
	EEJ	Exons 27-28	Ubr-201	-	ns	0.0029
	E	Exon 5	Ubr-201	Cassette Exon	ns	0.0075
	E	Exon 1	Ubr-205	Intron Retention	0.0074	ns
<i>Uchl5</i>	EEJ	Exons 1-2	Uchl5-201	-	0.0083	ns
	E	Exon 11	Uchl5-201	Alt 5' Donor Site	ns	0.0008
<i>Wrn</i>	EEJ	Exons 12-13	Wrn-201	-	0.0061	ns
	E	Exon 21	Wrn-201	Cassette Exon	ns	0.0057

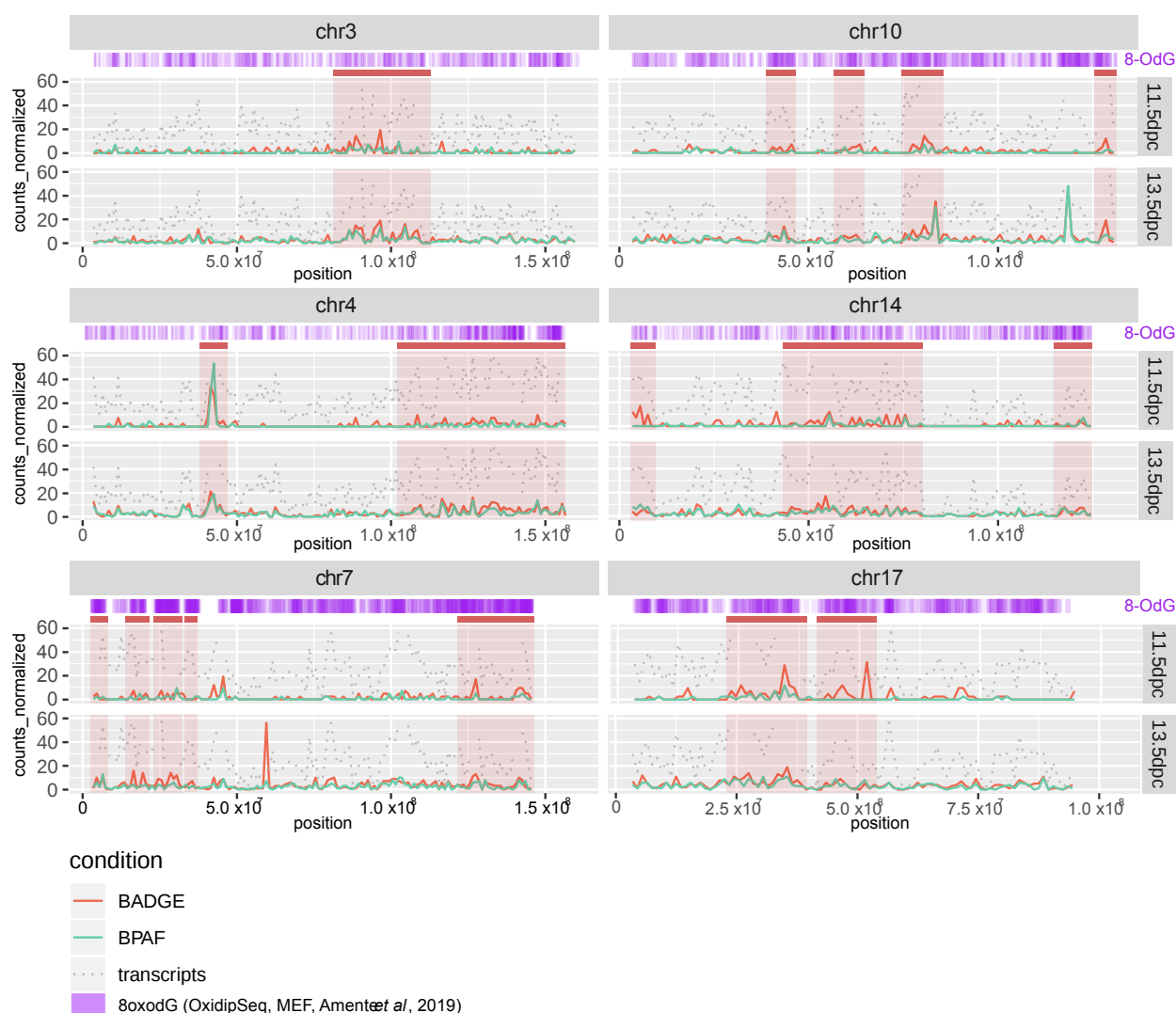
335 Some of the differentially spliced meiotic genes retrieved in both bisphenols exhibit the same  
336 splicing events such as *Smc4*, a condensin protein (Table 2 in red, Figure 5C). The presence of an  
337 alternative 3' acceptor sites in the first exon allows the production of different forms of *Smc4*  
338 transcripts containing or not a truncated exon 1 as observed in the *Smc4-202* and *Smc4-201*  
339 variants respectively. Using specific primers of the truncated/spliced region of the first exon and of  
340 the core/unspliced region of the transcript, we quantified by QPCR the relative abundance of the

339 mRNAs containing a long first exon. In BADGE as in BPAF -treated germ cells, we observed a  
340 significant decrease in the abundance of the long form with a corresponding increase of the  
341 truncated form of this first exon (Figure 5C). While we retrieved the same affected genes in  
342 BADGE and BPAF treated germ cells, the precise differential splicing events differs between  
343 conditions as observe for meiotic gene set (Table 2 in black). In BADGE -treated germ cells, we  
344 identified a differentially specific event occurring in the exon 38 of *Sycp2*, a component of the  
345 synaptonemal complex, due to alternative 3' acceptor sites (Table 2). These sites lead to the  
346 production of two types of variants with a complete or a truncated exon as observed in *Sycp2-201*  
347 and *Sycp2-202* transcripts. QPCR quantification revealed a significant increase in the relative  
348 abundance of the truncated form of the exon 38 only after BADGE exposure (Figure 5D).  
349 Genes differentially spliced in BPAF or BADGE conditions were not preferentially differentially  
350 expressed compared to others genes (Supplementary Figure 4). As observed with non-spliced  
351 genes, less than 8 % of spliced genes were also differentially expressed in BPAF or BADGE  
352 conditions. Interestingly, we observed closer transcription behaviors after BPAF or BADGE  
353 exposure of differentially spliced genes in comparison to non-differentially spliced genes randomly  
354 chosen (Supplementary Figure 4). This observation suggests a common alteration impacting the  
355 transcriptional response and RNA splicing after BADGE and BPAF exposure.



356 **Supplementary Figure 4:** 2d density plot between BADGE and BPAF condition of the differential  
357 expression (Log2FC) of differentially spliced genes in BADGE or BPAF condition. The plot area is  
358 divided in 200 hexagons and the color of the hexagon correspond to number of genes inside the  
359 hexagon. A simple random sampling of 3543 non differentially spliced genes (maximal number of  
360 differentially spliced genes) was used to represent transcriptional behavior after BADGE or BPAF  
361 exposure of non differentially spliced genes.

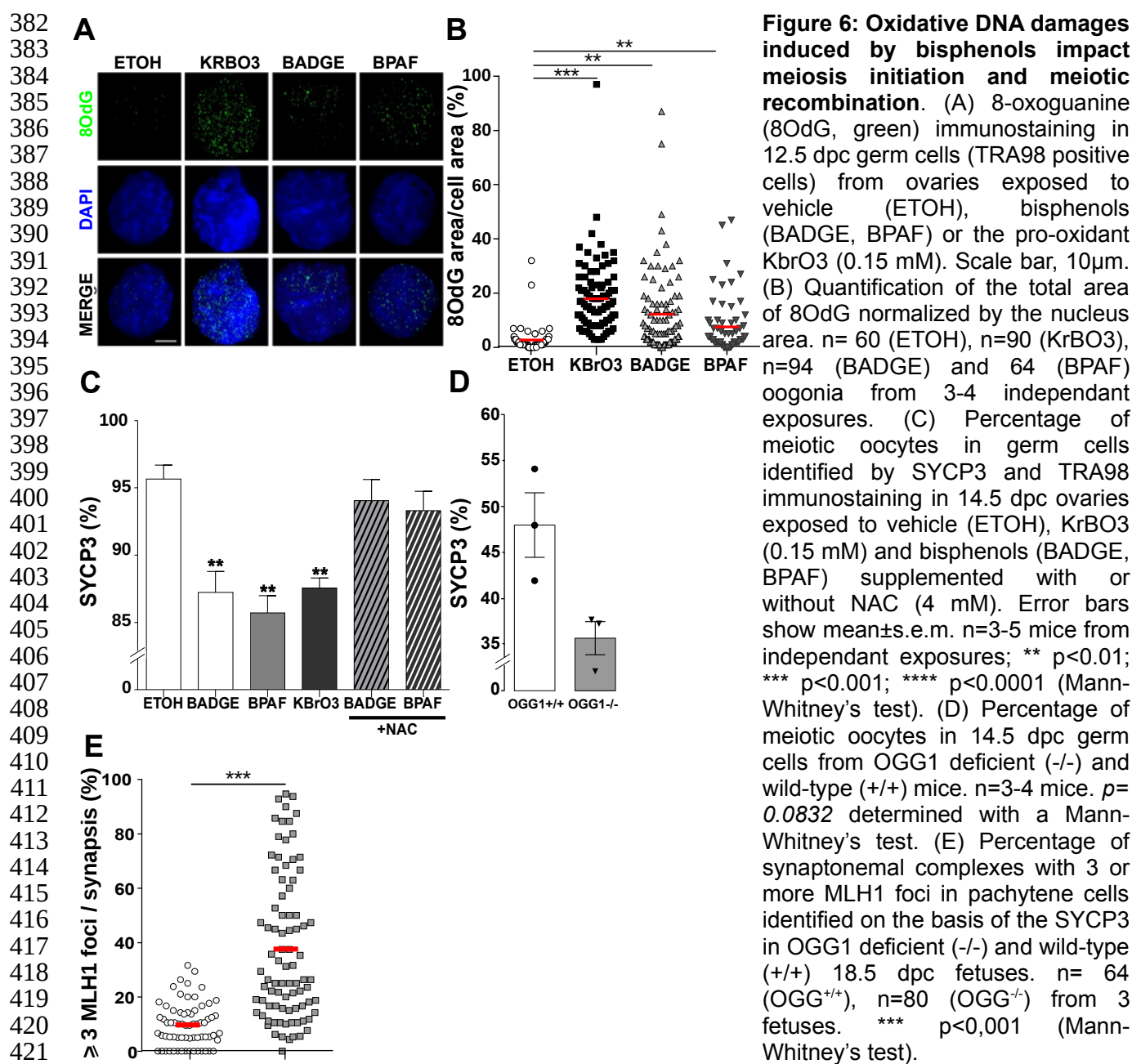
# BADGE or BPAF fetal exposures increase oxidative DNA damages impairing meiosis initiation.



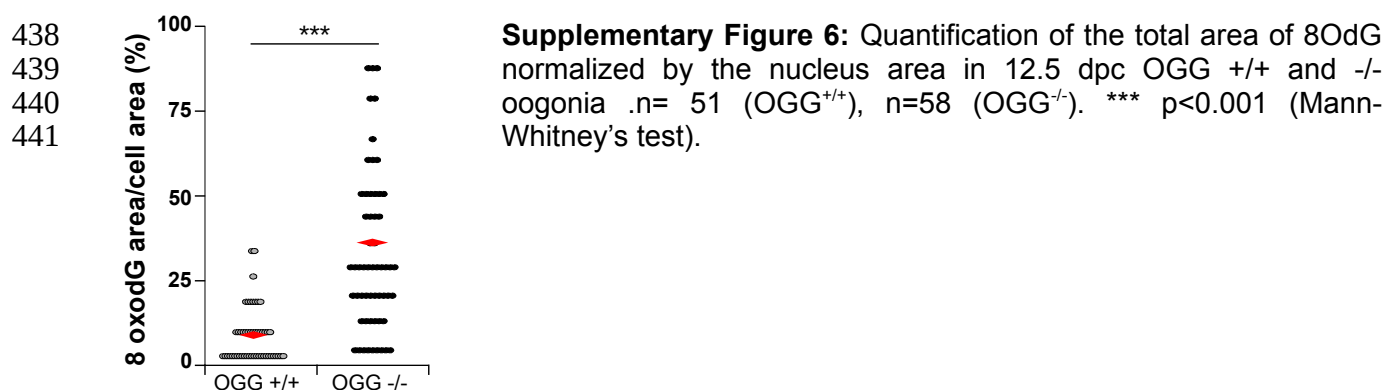
**Supplementary Figure 5.** Genome mapping on selected chromosomes (Chr 3, 4, 7, 10, 14, 17) of the DEGs in BPAF (red line) and BADGE (green line) conditions. The sum of the filtered genes per megabase (1000000 bases) was reported according to their location on the chromosome. Grey dotted line represent the sum of the total genes referenced in the murine genome. Purple line correspond to the mapping of the OxiDIP-Seq signal profiles retrieved in the Amente et al publication (Amente et al., 2019).

As BPA is a well-known oxidative stress generator in germ cells and other cell types we speculated that the formation of oxidative DNA damage such as 8-OdG might explain common transcriptional responses and RNA splicing after BADGE or BPAF exposure. Indeed, it is well known that the formation of oxidative DNA damages such as 8-OdG alters gene expression (Ba et Boldogh 2018). Using Oxidip-seq data obtained by Amente et al (Amente et al. 2019) on mouse embryonic

fibroblasts (MEF), we observed that DEGs genes could overlap with DNA regions susceptible to be oxidized (Supplementary Figure 5). Therefore, we analyzed the induction of oxidative DNA damages in response to bisphenols in 12.5 dpc proliferative oogonia by detection of 8-OdG (Figure 6A-B). As a positive control, we added the pro-oxidant potassium bromate (KBrO<sub>3</sub>) in drinking water from 10.5 dpc. As observed after KBrO<sub>3</sub> exposure, bisphenols-exposed PGCs showed a significant increase in 8-OdG when compared to the vehicle-treated germ cells (Figure 6B).



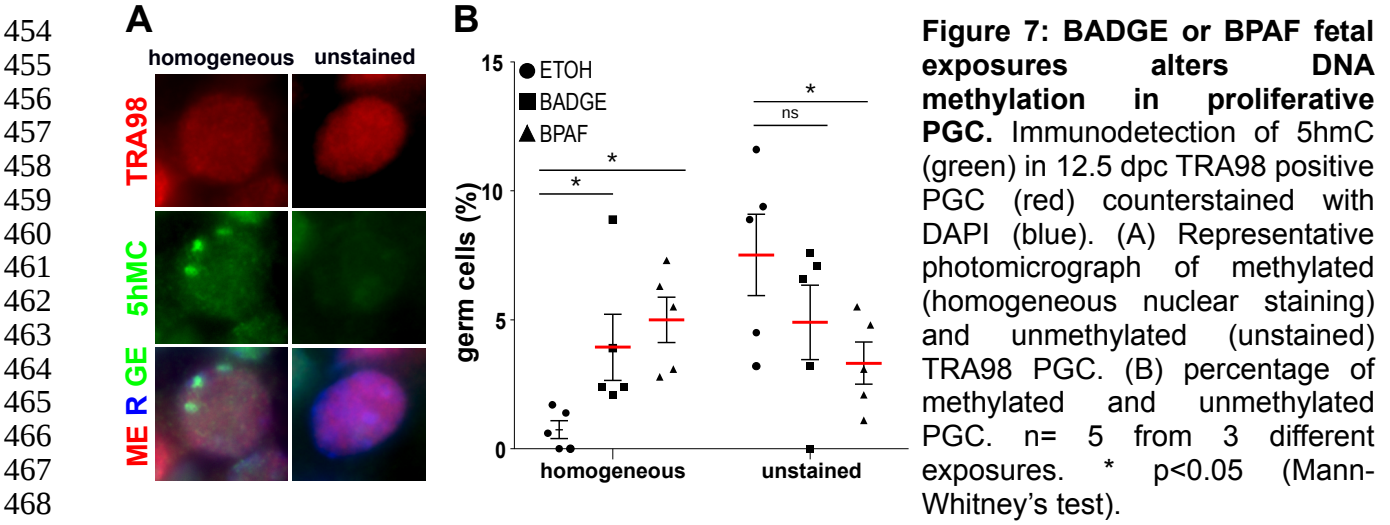
To explore the relationship between meiosis initiation delay and oxidative stress, we quantified meiosis initiation in KBrO<sub>3</sub> treated ovaries at 14.5 dpc. KBrO<sub>3</sub> exposure significantly decreased the proportion of meiotic oocytes (SYCP3 positive cells; Figure 6C). On the contrary, when we treated pregnant mice with bisphenols supplemented with the antioxidant N-acetylcysteine (NAC) to pregnant mice, we restored the percentage of oocytes to that of vehicle treated (ETOH) 14.5 dpc ovaries. To further assess the impact of oxidative lesions, we used mice deficient for OGG1, a DNA glycosylase involved in the removal of oxidative DNA damage through the Base Excision Repair (BER). *Ogg1*<sup>-/-</sup> mice showed increased levels of 8-OdG in proliferative 12.5 dpc oogonia in comparison to *Ogg1*<sup>+/+</sup> mice (Supplementary Figure 6). The lack of OGG1 also impaired meiosis initiation as we observed a decreasing trend of oocyte number at 14.5 dpc (48.0% ± 3.5, *Ogg1*<sup>+/+</sup> vs 35.7% ± 1.8, *Ogg1*<sup>-/-</sup>, p=0.0832; Figure 6D). To link oxidative DNA damage and recombination events, we quantified the number of MLH1 foci at 18.5 dpc in OGG1 deficient mice. Interestingly, as observed for bisphenols treated mice, the number of MLH1 foci was significantly increased in the mutant when compared to wild type mice (Figure 6E). Taken together these data reveal that bisphenols induce oxidative DNA damages which in turn could delay fetal meiosis and induce recombination defects.



#### **BADGE or BPAF fetal exposures alter DNA demethylation in PGCs.**

BPA has been reported to alter DNA methylation in various cell types and removal of DNA methylation is a mandatory event in proliferative PGC to allow later the proper expression of the meiotic program(Anderson et al., 2012; Chao et al., 2012; Hargan-Calvopina et al., 2016b; Yamaguchi et al., 2012). For this reason, we quantified the proportion of methylated/pluripotent

PGC compared to unmethylated/differentiating PGC by immunodetection in 12.5 dpc bisphenols exposed and unexposed ovaries of the 5-hydroxymethylCytosine (5hmC), the first intermediate form during active demethylation (Figure 7A). After bisphenols exposure, we observed an enrichment of methylated germ cells with a global staining (homogeneous staining) of 5hmC in the nucleus in TRA98 cells (Figure 7B). This result suggests that bisphenols exposure alters or delays the DNA demethylation in PGC increasing the proportion of methylated germ cells compared to unmethylated ones.



## 469 Discussion

470 Woman's reproductive pathologies include the ovarian dysgenesis syndrome that is defined as a  
 471 precocious alteration of ovarian function and mostly associated with premature ovarian  
 472 insufficiency, anovulation and/or pregnancy loss in the adulthood (Buck Louis et al., 2011). Oocyte  
 473 aneuploidy is strongly associated with these reproductive failures and growing evidences suggest  
 474 that fetal exposure to endocrine disruptors such as Bisphenol A (BPA) can cause female  
 475 reproductive defect (Johansson et al., 2017). In Vertebrates and Invertebrates species, exposure to  
 476 BPA induces transcription defect of meiotic genes, alters frequency of MLH1 foci and chiasmata  
 477 leading to chromosome missegregation during meiotic resumption (Allard & Colaiácovo, 2010a;  
 478 Brieno-Enriquez et al., 2012; Brieño-Enríquez et al., 2011; P. A. Hunt et al., 2012; Patricia A. Hunt  
 479 et al., 2003; Lawson et al., 2011; Susiarjo et al., 2007). Because BPA has been restricted and  
 480 regulated in many countries, BPA alternatives have been introduced into industrial products  
 481 increasing the exposure to other bisphenols such as BPAF and BADGE. Exposure to BADGE and  
 482 BPAF can be comparable to BPA exposure. A recent study has reported comparable median  
 483 concentrations of BPA and BADGE hydrated derivatives in human plasma collected from New York  
 484 City individuals (7.15 ng/ml for BADGE·2H<sub>2</sub>O and 2.26 ng/ml for BADGE·H<sub>2</sub>O versus 1.77 ng/ml for  
 485 BPA) likely due to similar exposure source to BPA (ie. from epoxy coatings into canned food) (L.  
 486 Wang et al., 2015). In China, BPAF mean concentration in human plasma is 0.073 ng/mL versus  
 487 0.4 ng/ml for BPA in the same samples from 81 individuals in general population (Jin et al., 2018).  
 488 For this reason, we investigated the consequences of BPAF and BADGE exposure on female germ  
 489 cell differentiation. Although BPAF concentration detected in human samples is lower than the one  
 490 of BADGE or BPA, we chose to expose mice by drinking water to BADGE or BPAF at the same  
 491 concentrations (ie 10μM). This allows to compare BPAF and BADGE and to compare our results to  
 492 previous studies, including ours, that used BPA at environmentally doses (Eladak et al., 2018). In  
 493 the present study, we exposed pregnant mice to bisphenols from 10.5 to 18.5 dpc. The  
 494 concentration of total BPAF detected in the plasma of the pregnant mice was of the a same order  
 495 of magnitude (5.96 ± 0.78 ng/ml) than the one we previously observed for BPA (Eladak et al.,  
 496 2018).

497 As observed for BPA, fetal exposure to BPAF or BADGE induces subtle oocyte defects during fetal  
498 life leading to aneuploidy at adulthood. We observed changes in expression levels of meiotic  
499 genes during meiosis initiation, and a modification of the frequency of MLH1 foci during  
500 pachynema and of chiasmata in diplonema leading to oocyte aneuploidy after meiotic division.  
501 Thus, we demonstrate that BPAF or BADGE seem as much harmful as BPA with regard to their  
502 deleterious effect on oogenesis.

503 Until now the modality of the action of BPA on meiosis remains unclear. Numerous evidences  
504 highlight a temporal window of oocyte vulnerability during fetal life, specifically before and during  
505 meiotic prophase I (Brieno-Enriquez et al., 2012; P. A. Hunt et al., 2012; Lawson et al., 2011;  
506 Susiarjo et al., 2007). Because consequences are mostly detectable in later steps it was difficult to  
507 determine the precise cellular target (*ie.* PGC or oocyte) of BPA. This questioned whether the  
508 bisphenol-induced meiotic failure originated from alterations that occurred during the differentiation  
509 of the PGC or during meiotic prophase I. In this study, we showed that exposure to bisphenols  
510 before meiotic prophase I affected crossover frequency. Therefore, this observation demonstrates  
511 that alterations induced by BPAF and BADGE in PGC alters the establishment of the meiotic  
512 program.

513 Proper establishment and orchestration of the meiotic program are essential to ensure a correct  
514 regulation of crossover distribution [57]. The establishment of prophase I requires two events:  
515 acquisition of meiotic competence and initiation of the meiotic program (Soh et al., 2015). Meiotic  
516 competence is acquired after PGCs colonization. Migratory PGCs have a genomic program  
517 associated with stemness and express pluripotent genes. In the gonad, at 10.5 dpc, PGCs switch  
518 off the pluripotency program and activate genes involved in gametogenesis. DAZL, a germ cell-  
519 specific RNA binding protein, binds germ cell specific mRNA and promotes the stabilization of  
520 meiotic mRNA allowing the initiation of the meiotic program (Atala, 2012; Hu et al., 2015; Kato et  
521 al., 2016; Nicholls et al., 2019). Our transcriptomic analyses revealed that bisphenol exposure  
522 alters the acquisition of the gametogenic competence and the initiation of the meiotic program.  
523 First, bisphenol exposure seems to induce a failure or a delay on the switch from pluripotency to

524 gametogenesis/meiosis competence. This is illustrated by a global down-regulation of meiosis  
 525 associated genes such as *Sycp1&3* and *Hormad2* and an up-regulation of pluripotency associated  
 526 genes such as *Msx1* and *Gata4*. Second, bisphenols exposure also impacts the initiation of the  
 527 meiotic program at 13.5 dpc as illustrated by the up-regulation of meiotic genes. These  
 528 observations are consistent with previous studies on the effect of BPA on human and murine  
 529 meiosis initiation (Houmard et al., 2009; Lawson et al., 2011). However, it is unclear whether the  
 530 up-regulation of meiotic genes induced by bisphenols is the consequence of the PGC  
 531 differentiation delay observed earlier, or a real induction of gene expression and/or RNA  
 532 stabilization. Indeed, numerous meiotic genes such as *Stra8* or *Rec8* are drastically down-  
 533 regulated just after meiosis onset. Therefore, a delay of meiosis initiation would lead us to observe  
 534 a higher level of expression of some meiotic transcripts (Soh et al., 2015). Moreover, bisphenol  
 535 exposure also induced a global alteration of splicing events during this step. Recent studies have  
 536 highlighted the role of mRNA splicing on the mitosis to meiosis transition in male and female germ  
 537 cells and lack of splicing regulators in male germ cells leads to meiotic defects (Liu et al., 2017;  
 538 Naro et al., 2017; Schmid et al., 2013; J. Wang et al., 2019). In consequences, minor modifications  
 539 of the splicing of meiotic genes after bisphenols exposure could impact meiosis. As observed for  
 540 BPA exposure, changes in level of gene expression were subtle but, interestingly, we observed  
 541 common transcriptional signature between BPAF and BADGE suggesting common bisphenol  
 542 molecular targets.

543 Transcriptional modifications observed after bisphenol exposure impacted the transition from  
 544 mitosis to meiosis and were certainly the origin of the observed delay of meiosis initiation and  
 545 progression, the abnormal distribution of MLH1 foci but also the cause of folliculogenesis  
 546 alterations (ie.MOF, follicle number). Indeed, the initiation of follicle assembly requires completion  
 547 of meiotic prophase and any delay in meiotic progression could interfere with this process (Chao et  
 548 al., 2012; A. Paredes et al., 2005; H.-Q. Zhang et al., 2012). Thus all these events may be related  
 549 forming a cascade resulting from the early alteration of the establishment of the meiotic program in  
 550 PGC.

551 Interestingly, common cellular (*ie* MLH1 and chiasmata distribution and MOF) and transcriptional  
552 meiotic signatures observed after bisphenols exposure and other pollutants such as phthalates in  
553 multiple organisms suggest a common mechanism of action of these molecules (Allard &  
554 Colaiácovo, 2010b; Cuenca et al., 2020; Gely-Pernot et al., 2017; Parodi et al., 2015; Shin et al.,  
555 2019; Susiarjo et al., 2007; Tu et al., 2019). In this study, we propose oxidative stress as an new  
556 player involved in bisphenol response that could impair the PGC differentiation. One of the major  
557 targets of reactive oxygen species is the DNA, and 8OdG is the most prominent lesion in the  
558 genome (Ba & Boldogh, 2018). We showed that bisphenol exposure quickly induces the formation  
559 of this oxidative DNA lesion in proliferative germ cells. Interestingly, analyzing the genomic  
560 landscape of oxidative DNA damage revealed a specific susceptibility to oxidation in genomic  
561 regions harboring genes differentially expressed after bisphenol exposure. It is well known that  
562 oxidative DNA damages can modulate gene expression directly or indirectly. First, oxidative DNA  
563 damage induce antioxidant and inflammatory transcriptional responses and recruiting DNA repair  
564 proteins (Hörandl & Hadacek, 2013; Pan et al., 2016). Second, oxidized guanine biases the  
565 recognition of methylated CpG dinucleotides and alters the dynamic of DNA demethylation (Gruber  
566 et al., 2018; Pan et al., 2016). Interestingly, acquisition of the meiotic competence is completely  
567 dependent on an intensive germinal DNA demethylation (Hargan-Calvopina et al., 2016b;  
568 Yamaguchi et al., 2012). In this study, we observed that bisphenols exposure interferes with DNA  
569 demethylation and could be the consequence of the presence of oxidative DNA damages. The  
570 presence of 8OdG has also post-transcriptional consequences and could alter splicing events. Pre-  
571 mRNA splicing requires the identification of specific 5' donor and 3' acceptor sites. The 5' and 3'  
572 splicing sites mostly begin with dinucleotide GT(U) and end with dinucleotide AG that allows the  
573 major 5'\_3' combination GT-AG (Calvello et al., 2013). Incorporation of the wrong base within these  
574 splicing signals would lead to an alteration of the fidelity of mRNA splicing. In mammalian cells,  
575 unrepaired DNA lesions such as 8OdG on the transcribed strand is a source of transcriptional  
576 mutagenesis. Unrepaired 8OdG leads to a single-nucleotide substitution in the 3' or 5' splice site  
577 subsequently resulting mostly in exon skipping and altering the protein product as it has been  
578 observed in the context of Ogg1 deficiency (J. A. Paredes et al., 2017). For these reasons, we

579 speculated that induction of oxidative stress by bisphenols could be responsible of observed  
580 transcriptional alteration as well as RNA splicing modification during meiosis initiation leading to  
581 prophase I defects. This is confirmed after specific induction of oxidative DNA damages in  
582 proliferative germ cell. Indeed, in KrBO3-treated ovaries and the timing of meiosis initiation is  
583 restored in presence of the antioxidant NAC. Moreover, in Ogg1 deficient mice, we also observed a  
584 delay of meiosis initiation and modification of MLH1 distribution in pachynema.

585 This study highlights the central role of oxidative DNA damage in the meiotic response after  
586 bisphenol exposure. Numerous past studies proposed a role for estrogen signaling in the meiotic  
587 responses (*ie* delay of meiotic progression, alteration of crossover distribution and aneuploidy) due  
588 to the effect of molecules with a xenoestrogenic potential (Cuenca et al., 2020; Susiarjo et al.,  
589 2007; Tu et al., 2019). Our hypothesis is in agreement with an involvement of estrogen signaling  
590 during this process as DNA binding by the estrogen receptor drives the local production of  
591 oxidative DNA damages via LSD1, a Lysine-specific histone demethylase 1, activity in promoter  
592 and enhancer regions (Perillo et al., 2008).

593 Current knowledge on the potential toxicological effects of BPA analogs is limited. We provide here  
594 proofs that endocrine disruptors such as bisphenols negatively impact the female germline causing  
595 oocyte defects with dramatic consequences such as aneuploidy. We also reveal that bisphenols  
596 effects are mediated by DNA oxidation. Numerous toxicological studies have linked prophase I  
597 alterations induced by pollutants, aneuploidy and folliculogenesis defect and, here, we  
598 demonstrated the central role of oxidative DNA damages in these ovarian reproductive failures  
599 (Cuenca et al., 2020; Gely-Pernot et al., 2017; P. A. Hunt et al., 2012; Susiarjo et al., 2013). This  
600 opens new research avenues considering DNA oxidation in the developing germline as the cause  
601 of adult reproductive defects. Such mechanism remains to be investigated in the human germline  
602 and could also be invoked for numerous pollutants, either considered or not as endocrine  
603 disruptors, whose reprotoxic potential has poorly been studied despite a strong oxidative potential.

## 604 **Experimental Procedures**

### 605 **Animals and gonads collection**

606 All animal care protocols and experiments were reviewed and approved by the ethics committee of  
 607 CETEA–CEA DSV (France, APAFIS 18515-2019011615312443v1) and followed the guidelines for  
 608 the care and use of laboratory animals of the French Ministry of Agriculture. Mice were maintained  
 609 in used polypropylene cage in standard and controlled photoperiod conditions (lights on from 8  
 610 a.m. to 8 p.m.) and had free access to tap water incubated in glass bottle and food. Males and  
 611 females were caged together overnight (one male for 2 females), and the presence of vaginal plug  
 612 was examined the following morning. The day following overnight mating is counted as 0.5 day  
 613 post conception (dpc). All mice were killed by cervical dislocation at 11.5 dpc, 12.5 dpc, 14.5 dpc,  
 614 18.5 dpc and 8 dpp or at 3 months after birth. For pregnant mice, fetuses were removed after  
 615 euthanasia from uterine horns before gonad isolation under a binocular microscope . The mice  
 616 used in this study were NMRI mice (Naval Maritime Research Institute) and OGG1 deficient  
 617 C57/Bl6 mice obtained from the production colony at our laboratory (Klungland et al., 2002).

### 618 **Exposition protocol**

619 The exposition protocol of this study is shown in Figure 2C and Supplementary Figure 2. BADGE  
 620 (CAS number 1675-54-3, Sigma D3415) and BPAF (CAS number 1478-61-1, Sigma 257591) were  
 621 dissolved in absolute ethanol (puriss, ≥99.8%). Final concentration of 10 μM (diluted in ethanol  
 622 0.1%) were provided in drinking water to isolated pregnant females from 10.5 dpc to 14.5 dpc for  
 623 short-term exposure (Supplementary Figure 2) or to 18.5 dpc for long-term exposure (Figure 2C).  
 624 The control group was given drinking water added with 0.1% ethanol. For transcriptomic analyses,  
 625 pregnant mice were euthanased at 11.5 dpc and 13.5 dpc to collect gonad for germ cell sorting. As  
 626 one adult mouse drinks 150 ml per kg body weight and per day, the evaluated daily intake of BPAF  
 627 and BADGE by treated mice is ~500 μg/kg/day. Internal BPAF concentration was evaluated. Total  
 628 BPAF was measured by gas chromatography coupled to tandem mass spectrometry (GC-MS/MS)  
 629 in the plasma of 18.5 dpc pregnant mice as previously described (Eladak et al., 2018) The mean ±  
 630 sem values in the plasma of BPAF group were 5.96 ± 0.78 ng/ml (n=4). As a comparison, he

631 'European Food Safety Authority (EFSA) stated that the NOAELs for BADGE and BPAF is 15 and  
632 30 mg/kg/d respectively <https://www.anses.fr/fr/system/files/CHIM2009sa0331Ra-1.pdf>. N-  
633 acetylcystein (NAC; Sigma A9165, 4 mM) and potassium bromate (KBrO<sub>3</sub>; Merck 1.04212.0250,  
634 0.15 mM) were also provided in water drink from day 10.5 dpc to the end of experiment.

### 635 **BrdU incorporation and detection in fetal ovaries**

636 For BrdU incorporation, 14.5 dpc ovaries were cultured in hanging drops with BrdU (1%). After  
637 three hours, ovaries were fixed in 4% paraformaldehyde and processed for histology.

### 638 **Histology and immunofluorescence on ovarian sections**

639 Protocols used have been described previously (Abby et al., 2016, Poulain et al., 2014). Briefly,  
640 fetal and adult ovaries were fixed overnight in Bouin's fluid. After being dehydrated and embedded  
641 in paraffin, gonads were cut into 5-µm-thick sections. Sections were then mounted on slides for  
642 haematoxylin and eosin coloration. Germ cells on each section were identified on the basis of their  
643 histological features, as previously described and oogonia were identified as small cells with high  
644 nucleocytoplasmic ratio and the presence of prominent nucleoli. Meiotic cells displayed markedly  
645 condensed chromatin, forming distinct fine threads with a beaded appearance at the leptotene  
646 stage, and a characteristic criss-cross of coiled chromosome threads at the zygotene stage, while  
647 oocytes reaching the diplotene stage (naked or enclosed in follicle) had an increased size with the  
648 reformation of a single nucleolus. The Histolab analysis software (Microvision Instruments, Evry,  
649 France) was used for counting. Immunostaining were performed on sections from fetal gonads  
650 (12.5 and 14.5 dpc) fixed overnight in 4% paraformaldehyde (PFA). Sections were submitted to  
651 antigen retrieval with citrate buffer (pH 6) and then blocked in Normal Horse Serum (Impress HRP  
652 Reagent Kit MP-7402) or 2% gelatin, 0.05% tween, 0.2% BSA for one hour before adding  
653 antibodies. Primary antibodies used in this study were as follows: monoclonal mouse anti-5mC  
654 (abcam ab10805, 1:100), monoclonal rabbit anti-Stra8 (abcam ab49602; 1:1000), monoclonal rat  
655 anti-TRA98 (abcam ab82527, 1:500), and monoclonal mouse anti-SYCP3 (abcam ab97672, 1:500)  
656 antibodies were used. Specific donkey secondary antibodies conjugated with either Alexa Fluor

488 or 594 (1:500). BrdU detection in histological sections was performed with the Cell Proliferation kit (RPN20, GE Healthcare). Slides were mounted with Vectashield medium. Images acquisition was accomplished with a Leica DM5500 B epifluorescence microscope (Leica Microsystems) equipped with a CoolSNAP HQ2camera (Photometrics) and ImageJ Software. Images were analyzed with the Image J software.

## **Immunofluorescence on chromosome spreads**

Chromosome spreads were prepared using fetal gonads (12.5 and 18.5 dpc). Fetal ovaries were lacerated on precleaned/ready-to-use superfrost slides in 1X PBS, then they were supplemented with 0.2% sucrose before adding 1% paraformaldehyde/1% Triton. Slides were incubated for 1 h at room temperature in a humid chamber and then dried under a hood and then washed two times for 10 min with 0.4% H<sub>2</sub>O/Photoflow (Sigma-Aldrich). Slides were stained immediately or dried and stored at -20 °C. Spreaded 12.5 dpc oogonia were rehydrated in PBS, denaturated with 2N HCl for 45 minutes and then neutralized with a 50 mM Tris-HCl (pH8.8) solution. Slides were washed three times in PBS-0.1% Triton and then incubated in blocking solution (PBS with 0.1% triton and 5% donkey serum) before adding antibodies. Monoclonal mouse anti-8-OHdG (Eurobio MOG-020P, 1:200) and monoclonal rat anti-TRA98 antibodies were diluted in blocking solution and incubated overnight. Spreaded 18.5 dpc oocytes were blocked in blocking solution before adding antibodies. Monoclonal mouse anti-MLH1 (BD Bio sciences, G16815, 1:50) and monoclonal rabbit anti-SYCP3 (Novus, NB300232, 1:500) antibodies were diluted in blocking solution and incubated overnight. After 3 washes, donkey secondary antibodies conjugated with either Alexa Fluor 488 or 594 (1:500) were added. Metaphase I and II oocytes were obtained with adult ovaries (3 months old females). Ovaries were lacerated in M2 medium (Sigma M7167) and oocytes at germinal vesicle stage were collected and cultured for five hours (for metaphase I) or sixteen hours (for metaphase II) in M16 medium, covered with mineral oil. Oocytes at Germinal Vesicle Breakdown (GVBD) stage (for metaphase I) or with the first polar globule expulsion (for metaphase II) were transferred into a drop of Tyrode solution for zona pellucida removal. They were spread on Teflon printed diagnostic slides in water with 3mM DTT, 0.15% Triton and 0.6% paraformaldehyde. Slides were

684 then dried and stored at  $-20^{\circ}\text{C}$ . Slides were washed three times in PBS and then incubated in  
685 blocking solution (PBS with 2% gelatin, 0.05% tween, 0.2% BSA) before adding monoclonal  
686 human anti-CREST (1:1000) antibody overnight. After 3 washes, goat anti-human secondary  
687 antibodies conjugated with Alexa Fluor 488 (1:500) were added. Slides were mounted with  
688 Vectashield with or without DAPI medium. Images were processed and specific structures were  
689 quantified with the ImageJ software (Cell Counter plugin).

## 690 **Germ cell isolation**

691 11.5 dpc and 13.5 dpc germ cell isolation using SSEA-1 antigen was performed as previously  
692 described (Guerquin et al, 2015). Briefly, fetal ovaries were dissociated using trypsin solution. Cells  
693 are incubated with anti-SSEA (1/5, anti SSEA1 monoclonal antibody DSHB) and then incubated  
694 with a microbead-linked donkey anti-mouse IgM antibody (Miltenyi Biotec). Then, cells were  
695 applied onto an MS+ column (Miltenyi Biotec) and the positive fraction was flushed after the  
696 removal of the magnet.

## 697 **Affymetrix sample preparation**

698 After isolation, cells were centrifuged and resuspended in RNeasy lysis buffer. RNA was extracted  
699 using Qiagen Rneasy miniKit as recommended by the manufacturer. Total RNA concentration and  
700 RNA integrity was monitored by electrophoresis (Agilent Bioanalyzer; RNA 6000 Pico Assay).  
701 Three pools of cells from 20-30 fetus (5 independent exposures) were used for differential  
702 expression analyses. Gene expression analysis was conducted using Mouse Clariom S array  
703 (Thermo Fisher) at 11.5 dpc and a Mouse Clariom D array at 13.5 dpc (Thermo Fisher). 500  $\mu\text{g}$  of  
704 total RNA were processed according to the manufacturer. Raw data were generated and controlled  
705 with Expression console (Affymetrix) at the Genomic's platform (Institut Cochin, Paris) for 11.5 dpc  
706 analyses and at the CEA for 13.5 dpc analyses.

## 707 **Microarray analysis**

708 For gene expression analyses (11.5 dpc or 13.5 dpc), R oligo package 1.42.0 (Carvalho & Irizarry,  
709 2010) was used for probeset annotation with expression summarized at the transcript level and  
710 robust multi-array averaging-normalized. Differential expression testing was conducted by ANOVA  
711 after linear model fitting of expression intensities with the limma R package. Microarray expression  
712 values are represented as log(2) normalized intensities. Differentially expressed genes (DEG) was  
713 filtered with a  $\log_{2}FC \geq 0.5$  and a  $pvalue < 0.05$ . For 13.5 dpc RNA splicing analyses, the  
714 expression was summarized at the exon level. Samples were analyzed using default parameters.  
715 An alternative splicing event was defined as a differentially expressed exon with at least a 1 Log  
716 fold change in expression, at a  $pvalue$  of  $< 0.05$ . Downstream analyses were performed with R  
717 version 3.5.0 on a CentOS Linux 7 system (64-bit). Enrichment analyses were performed using  
718 ClusterProfiler, a R package for comparing biological themes among gene clusters (G. Yu et al.,  
719 2012).

## 720 **Splicing variant detection by quantitative PCR**

721 Total RNA from isolated germ cells was extracted using the RNeasy minikit (QIAGEN, Valencia,  
722 CA, USA). cDNA was obtained by reverse transcription using the high capacity kit (Applied  
723 Biosystems, Foster City, CA, USA) according to the manufacturer's instructions. Set of primers  
724 specific to the truncated/spliced region and reference primers located to the core/unspliced of the  
725 transcript were used to quantify the region of splicing using 2 delta delta CT methods.

## 726 **Statistical analysis**

727 All data are presented as means  $\pm$  s.e.m. Statistical analyses were performed using Graphpad  
728 software and the R version 3.5.0. All individual biological replicates were randomly sampled from 3  
729 independent exposures (for bisphenols exposure). The statistical significance in the difference  
730 between control and bisphenols-treated data were evaluated using the non-parametric test Mann-  
731 Whitney. Statistical significance was set as  $p < 0.05$ .

## 732 **Data and Code Availability**

733 Datasets are available at the European Bioinformatics Institute under accession n° (E-MTAB-  
734 9344). The authors declare that the data supporting the findings of this study and custom code  
735 generated for the manuscript are available from the Lead Contact upon request.

## 736 **Acknowledgments**

737 We are grateful to Katja Wassmann, Damien Cladière and Eulalie Buffin for discussion and  
 738 suggestions and technical help for metaphase I and II preparation. We also thank A. Gouret and A.  
 739 Leliard for her skillful secretarial assistance. We also thank the team within the animal housing  
 740 facility at the iRCM. For affymetrix data, we thank Sébastien Jacques and Angeline Duché from  
 741 Genom'ic (institut Cochin). For BPAF concentration in serum samples, we thank Jean-Philippe  
 742 Antignac from LABERCA (Oniris, INRAE, Nantes). This research was supported by the ADEME  
 743 (French Environment & Energy Management Agency), ANSES (French Agency for Food,  
 744 Environmental and Occupational Health & Safety) Université de Paris and INSERM. S.A. were  
 745 supported by a fellowship from the Ministère de l'Enseignement et Recherche.

## 746 **Author Contributions**

747 Conceptualization: M.J.G, G.L., V.R.F, A.C, J.P.R, E.M and R.H ; Methodology: S.A., M.J.G, A.C,  
 748 J.P.R, E.M; Validation: S.A., D.M., M.W and S.M.; Formal Analysis: M.J.G and S.A. Investigation:  
 749 S.A., D.M., M.W and S.M; Resources: A.C. and J.P.R; Data Curation: M.J.G.; Writing –Original  
 750 Draft: S.A. and M.J.G.; Writing –Review & Editing: S.A., G.L., V.R.F, A.C, J.P.R, E.M and R.H.  
 751 Visualization: S.A. and M.J.G. Supervision: M.J.G, V.R.F and G.L. Project Administration: M.J.G,  
 752 V.R.F and G.L. Funding Acquisition: M.J.G, V.R.F and G.L.

## 753 **Declaration of Interests**

754 The authors declare no competing interests

## 755 References

- Allard, P., & Colaiácovo, M. P. (2010a). Bisphenol A impairs the double-strand break repair machinery in the germline and causes chromosome abnormalities. *Proceedings of the National Academy of Sciences of the United States of America*, 107(47), 20405-20410. <https://doi.org/10.1073/pnas.1010386107>
- Allard, P., & Colaiácovo, M. P. (2010b). Bisphenol A impairs the double-strand break repair machinery in the germline and causes chromosome abnormalities. *Proceedings of the National Academy of Sciences of the United States of America*, 107(47), 20405-20410. <https://doi.org/10.1073/pnas.1010386107>
- Amente, S., Di Palo, G., Scala, G., Castrignanò, T., Gorini, F., Coccozza, S., Moresano, A., Pucci, P., Ma, B., Stepanov, I., Lania, L., Pelicci, P. G., Dellino, G. I., & Majello, B. (2019). Genome-wide mapping of 8-oxo-7,8-dihydro-2'-deoxyguanosine reveals accumulation of oxidatively-generated damage at DNA replication origins within transcribed long genes of mammalian cells. *Nucleic Acids Research*, 47(1), 221-236. <https://doi.org/10.1093/nar/gky1152>
- Anderson, O. S., Nahar, M. S., Faulk, C., Jones, T. R., Liao, C., Kannan, K., Weinhouse, C., Rozek, L. S., & Dolinoy, D. C. (2012). Epigenetic responses following maternal dietary exposure to physiologically relevant levels of bisphenol A. *Environmental and Molecular Mutagenesis*, 53(5), 334-342. <https://doi.org/10.1002/em.21692>
- Ashley, T., Walpita, D., & de Rooij, D. G. (2001). Localization of two mammalian cyclin dependent kinases during mammalian meiosis. *Journal of Cell Science*, 114(Pt 4), 685-693.
- Atala, A. (2012). Re: Licensing of Gametogenesis, Dependent on RNA Binding Protein DAZL, as a Gateway to Sexual Differentiation of Fetal Germ Cells. *Journal of Urology*, 187(2), 764-765. <https://doi.org/10.1016/j.juro.2011.10.069>
- Ba, X., & Boldogh, I. (2018). 8-Oxoguanine DNA glycosylase 1: Beyond repair of the oxidatively modified base lesions. *Redox Biology*, 14, 669-678. <https://doi.org/10.1016/j.redox.2017.11.008>
- Bailey, A. S., Batista, P. J., Gold, R. S., Chen, Y. G., de Rooij, D. G., Chang, H. Y., & Fuller, M. T. (2017). The conserved RNA helicase YTHDC2 regulates the transition from proliferation to differentiation in the germline. *ELife*, 6. <https://doi.org/10.7554/eLife.26116>
- Brieno-Enriquez, M. A., Reig-Viader, R., Cabero, L., Toran, N., Martinez, F., Roig, I., & Garcia Caldes, M. (2012). Gene expression is altered after bisphenol A exposure in human fetal oocytes in vitro. *Molecular Human Reproduction*, 18(4), 171-183. <https://doi.org/10.1093/molehr/gar074>
- Brieño-Enriquez, M. A., Robles, P., Camats-Tarruella, N., García-Cruz, R., Roig, I., Cabero, L., Martínez, F., & Caldés, M. G. (2011). Human meiotic progression and recombination are affected by Bisphenol A exposure during in vitro human oocyte development. *Human Reproduction*, 26(10), 2807-2818. <https://doi.org/10.1093/humrep/der249>
- Buck Louis, G. M., Cooney, M. A., & Peterson, C. M. (2011). The ovarian dysgenesis syndrome. *Journal of Developmental Origins of Health and Disease*, 2(1), 25-35. <https://doi.org/10.1017/S2040174410000693>
- Calvello, R., Cianciulli, A., & Panaro, M. A. (2013). Conservation/Mutation in the splice sites of cytokine receptor genes of mouse and human. *International Journal of Evolutionary Biology*, 2013, 818954. <https://doi.org/10.1155/2013/818954>
- Carvalho, B. S., & Irizarry, R. A. (2010). A framework for oligonucleotide microarray preprocessing. *Bioinformatics (Oxford, England)*, 26(19), 2363-2367. <https://doi.org/10.1093/bioinformatics/btq431>
- Chao, H.-H., Zhang, X.-F., Chen, B., Pan, B., Zhang, L.-J., Li, L., Sun, X.-F., Shi, Q.-H., & Shen, W. (2012). Bisphenol A exposure modifies methylation of imprinted genes in mouse oocytes via the estrogen receptor signaling pathway. *Histochemistry and Cell Biology*, 137(2), 249-259. <https://doi.org/10.1007/s00418-011-0894-z>
- Cheng, E. Y., Hunt, P. A., Nalwai-Cecchini, T. A., Fligner, C. L., Fujimoto, V. Y., Pasternack, T. L., Schwartz, J. M., Steinauer, J. E., Woodruff, T. J., Cherry, S. M., Hansen, T. A., Vallente, R.

- U., Broman, K. W., & Hassold, T. J. (2009). Meiotic Recombination in Human Oocytes. *PLoS Genetics*, 5(9), e1000661. <https://doi.org/10.1371/journal.pgen.1000661>
- Chianese, R., Troisi, J., Richards, S., Scafuro, M., Fasano, S., Guida, M., Pierantoni, R., & Meccariello, R. (2017). Bisphenol A in reproduction: Epigenetic effects. *Current Medicinal Chemistry*, 24. <https://doi.org/10.2174/0929867324666171009121001>
- Cuenca, L., Shin, N., Lascarez-Lagunas, L. I., Martinez-Garcia, M., Nadarajan, S., Karthikraj, R., Kannan, K., & Colaiácovo, M. P. (2020). Environmentally-relevant exposure to diethylhexyl phthalate (DEHP) alters regulation of double-strand break formation and crossover designation leading to germline dysfunction in *Caenorhabditis elegans*. *PLoS Genetics*, 16(1), e1008529. <https://doi.org/10.1371/journal.pgen.1008529>
- Ding, Z.-M., Jiao, X.-F., Wu, D., Zhang, J.-Y., Chen, F., Wang, Y.-S., Huang, C.-J., Zhang, S.-X., Li, X., & Huo, L.-J. (2017). Bisphenol AF negatively affects oocyte maturation of mouse in vitro through increasing oxidative stress and DNA damage. *Chemico-Biological Interactions*, 278, 222-229. <https://doi.org/10.1016/j.cbi.2017.10.030>
- Eladak, S., Moison, D., Guerquin, M.-J., Matilionyte, G., Kilcoyne, K., N'Tumba-Byn, T., Messiaen, S., Deceuninck, Y., Pozzi-Gaudin, S., Benachi, A., Livera, G., Antignac, J.-P., Mitchell, R., Rouiller-Fabre, V., & Habert, R. (2018). Effects of environmental Bisphenol A exposures on germ cell development and Leydig cell function in the human fetal testis. *PLoS One*, 13(1), e0191934. <https://doi.org/10.1371/journal.pone.0191934>
- Ganesan, S., & Keating, A. F. (2016). Bisphenol A-Induced Ovotoxicity Involves DNA Damage Induction to Which the Ovary Mounts a Protective Response Indicated by Increased Expression of Proteins Involved in DNA Repair and Xenobiotic Biotransformation. *Toxicological Sciences*, 152(1), 169-180. <https://doi.org/10.1093/toxsci/kfw076>
- Gely-Pernot, A., Saci, S., Kernanec, P.-Y., Hao, C., Giton, F., Kervarrec, C., Tevosian, S., Mazaud-Guittot, S., & Smagulova, F. (2017). Embryonic exposure to the widely-used herbicide atrazine disrupts meiosis and normal follicle formation in female mice. *Scientific Reports*, 7(1), 3526. <https://doi.org/10.1038/s41598-017-03738-1>
- Gibert, Y. (Éd.). (2015). *Bisphenol A: Sources, risks of environmental exposure, and human health effects*. Nova Publishers.
- Gruber, D. R., Toner, J. J., Miears, H. L., Shernyukov, A. V., Kiryutin, A. S., Lomzov, A. A., Endutkin, A. V., Grin, I. R., Petrova, D. V., Kupryushkin, M. S., Yurkovskaya, A. V., Johnson, E. C., Okon, M., Bagryanskaya, E. G., Zharkov, D. O., & Smirnov, S. L. (2018). Oxidative damage to epigenetically methylated sites affects DNA stability, dynamics and enzymatic demethylation. *Nucleic Acids Research*, 46(20), 10827-10839. <https://doi.org/10.1093/nar/gky893>
- Hannigan, M. M., Zagore, L. L., & Licatalosi, D. D. (2017). Ptpb2 Controls an Alternative Splicing Network Required for Cell Communication during Spermatogenesis. *Cell Reports*, 19(12), 2598-2612. <https://doi.org/10.1016/j.celrep.2017.05.089>
- Hargan-Calvopina, J., Taylor, S., Cook, H., Hu, Z., Lee, S. A., Yen, M.-R., Chiang, Y.-S., Chen, P.-Y., & Clark, A. T. (2016a). Stage-Specific Demethylation in Primordial Germ Cells Safeguards against Precocious Differentiation. *Developmental Cell*, 39(1), 75-86. <https://doi.org/10.1016/j.devcel.2016.07.019>
- Hargan-Calvopina, J., Taylor, S., Cook, H., Hu, Z., Lee, S. A., Yen, M.-R., Chiang, Y.-S., Chen, P.-Y., & Clark, A. T. (2016b). Stage-Specific Demethylation in Primordial Germ Cells Safeguards against Precocious Differentiation. *Developmental Cell*, 39(1), 75-86. <https://doi.org/10.1016/j.devcel.2016.07.019>
- Hörandl, E., & Hadacek, F. (2013). The oxidative damage initiation hypothesis for meiosis. *Plant Reproduction*, 26(4), 351-367. <https://doi.org/10.1007/s00497-013-0234-7>
- Houmard, B., Small, C., Yang, L., Naluai-Cecchini, T., Cheng, E., Hassold, T., & Griswold, M. (2009). Global Gene Expression in the Human Fetal Testis and Ovary1. *Biology of Reproduction*, 81(2), 438-443. <https://doi.org/10.1095/biolreprod.108.075747>
- Hu, Y.-C., Nicholls, P. K., Soh, Y. Q. S., Daniele, J. R., Junker, J. P., van Oudenaarden, A., & Page, D. C. (2015). Licensing of Primordial Germ Cells for Gametogenesis Depends on Genital Ridge Signaling. *PLOS Genetics*, 11(3), e1005019. <https://doi.org/10.1371/journal.pgen.1005019>

- Hunt, P. A., Lawson, C., Gieske, M., Murdoch, B., Smith, H., Marre, A., Hassold, T., & VandeVoort, C. A. (2012). Bisphenol A alters early oogenesis and follicle formation in the fetal ovary of the rhesus monkey. *Proceedings of the National Academy of Sciences*, 109(43), 17525-17530. <https://doi.org/10.1073/pnas.1207854109>
- Hunt, Patricia A., & Hassold, T. J. (2008). Human female meiosis: What makes a good egg go bad? *Trends in Genetics: TIG*, 24(2), 86-93. <https://doi.org/10.1016/j.tig.2007.11.010>
- Hunt, Patricia A., Koehler, K. E., Susiarjo, M., Hodges, C. A., Ilagan, A., Voigt, R. C., Thomas, S., Thomas, B. F., & Hassold, T. J. (2003). Bisphenol A Exposure Causes Meiotic Aneuploidy in the Female Mouse. *Current Biology*, 13(7), 546-553. [https://doi.org/10.1016/S0960-9822\(03\)00189-1](https://doi.org/10.1016/S0960-9822(03)00189-1)
- Ishiguro, K.-I., Matsuura, K., Tani, N., Takeda, N., Usuki, S., Yamane, M., Sugimoto, M., Fujimura, S., Hosokawa, M., Chuma, S., Ko, M. S. H., Araki, K., & Niwa, H. (2020). MEIOSIN Directs the Switch from Mitosis to Meiosis in Mammalian Germ Cells. *Developmental Cell*, 52(4), 429-445.e10. <https://doi.org/10.1016/j.devcel.2020.01.010>
- Jin, H., Zhu, J., Chen, Z., Hong, Y., & Cai, Z. (2018). Occurrence and Partitioning of Bisphenol Analogues in Adults' Blood from China. *Environmental Science & Technology*, 52(2), 812-820. <https://doi.org/10.1021/acs.est.7b03958>
- Johansson, H. K. L., Svingen, T., Fowler, P. A., Vinggaard, A. M., & Boberg, J. (2017). Environmental influences on ovarian dysgenesis—Developmental windows sensitive to chemical exposures. *Nature Reviews Endocrinology*, 13(7), 400-414. <https://doi.org/10.1038/nrendo.2017.36>
- Jones, R. L., Lang, S. A., Kendzierski, J. A., Greene, A. D., & Burns, K. A. (2018). Use of a Mouse Model of Experimentally Induced Endometriosis to Evaluate and Compare the Effects of Bisphenol A and Bisphenol AF Exposure. *Environmental Health Perspectives*, 126(12), 127004. <https://doi.org/10.1289/EHP3802>
- Kato, Y., Katsuki, T., Kokubo, H., Masuda, A., & Saga, Y. (2016). Dazl is a target RNA suppressed by mammalian NANOS2 in sexually differentiating male germ cells. *Nature Communications*, 7(1), 11272. <https://doi.org/10.1038/ncomms11272>
- Kim, J. H., Sartor, M. A., Rozek, L. S., Faulk, C., Anderson, O. S., Jones, T. R., Nahar, M. S., & Dolinoy, D. C. (2014). Perinatal bisphenol A exposure promotes dose-dependent alterations of the mouse methylome. *BMC Genomics*, 15(1), 30. <https://doi.org/10.1186/1471-2164-15-30>
- Lam, I., & Keeney, S. (2015). Mechanism and Regulation of Meiotic Recombination Initiation. *Cold Spring Harbor Perspectives in Biology*, 7(1), a016634. <https://doi.org/10.1101/cshperspect.a016634>
- Lawson, C., Gieske, M., Murdoch, B., Ye, P., Li, Y., Hassold, T., & Hunt, P. A. (2011). Gene Expression in the Fetal Mouse Ovary Is Altered by Exposure to Low Doses of Bisphenol A1. *Biology of Reproduction*, 84(1), 79-86. <https://doi.org/10.1095/biolreprod.110.084814>
- Le Bouffant, R., Guerquin, M. J., Duquenne, C., Frydman, N., Coffigny, H., Rouiller-Fabre, V., Frydman, R., Habert, R., & Livera, G. (2010). Meiosis initiation in the human ovary requires intrinsic retinoic acid synthesis. *Human Reproduction*, 25(10), 2579-2590. <https://doi.org/10.1093/humrep/deq195>
- Liu, W., Wang, F., Xu, Q., Shi, J., Zhang, X., Lu, X., Zhao, Z.-A., Gao, Z., Ma, H., Duan, E., Gao, F., Gao, S., Yi, Z., & Li, L. (2017). BCAS2 is involved in alternative mRNA splicing in spermatogonia and the transition to meiosis. *Nature Communications*, 8, 14182. <https://doi.org/10.1038/ncomms14182>
- Nagaoka, S. I., Hassold, T. J., & Hunt, P. A. (2012). Human aneuploidy: Mechanisms and new insights into an age-old problem. *Nature Reviews. Genetics*, 13(7), 493-504. <https://doi.org/10.1038/nrg3245>
- Naro, C., Jolly, A., Di Persio, S., Bielli, P., Setterblad, N., Alberdi, A. J., Vicini, E., Geremia, R., De la Grange, P., & Sette, C. (2017). An Orchestrated Intron Retention Program in Meiosis Controls Timely Usage of Transcripts during Germ Cell Differentiation. *Developmental Cell*, 41(1), 82-93.e4. <https://doi.org/10.1016/j.devcel.2017.03.003>
- Nicholls, P. K., Schorle, H., Naqvi, S., Hu, Y.-C., Fan, Y., Carmell, M. A., Dobrinski, I., Watson, A. L., Carlson, D. F., Fahrenkrug, S. C., & Page, D. C. (2019). Mammalian germ cells are

- determined after PGC colonization of the nascent gonad. *Proceedings of the National Academy of Sciences of the United States of America*, 116(51), 25677-25687. <https://doi.org/10.1073/pnas.1910733116>
- Ottolini, C. S., Newnham, L., Capalbo, A., Natesan, S. A., Joshi, H. A., Cimadomo, D., Griffin, D. K., Sage, K., Summers, M. C., Thornhill, A. R., Housworth, E., Herbert, A. D., Rienzi, L., Ubaldi, F. M., Handyside, A. H., & Hoffmann, E. R. (2015). Genome-wide maps of recombination and chromosome segregation in human oocytes and embryos show selection for maternal recombination rates. *Nature Genetics*, 47(7), 727-735. <https://doi.org/10.1038/ng.3306>
- Pan, L., Zhu, B., Hao, W., Zeng, X., Vlahopoulos, S. A., Hazra, T. K., Hegde, M. L., Radak, Z., Bacsí, A., Brasier, A. R., Ba, X., & Boldogh, I. (2016). Oxidized Guanine Base Lesions Function in 8-Oxoguanine DNA Glycosylase-1-mediated Epigenetic Regulation of Nuclear Factor κB-driven Gene Expression. *Journal of Biological Chemistry*, 291(49), 25553-25566. <https://doi.org/10.1074/jbc.M116.751453>
- Paredes, A., Garcia-Rudaz, C., Kerr, B., Tapia, V., Dissen, G. A., Costa, M. E., Cornea, A., & Ojeda, S. R. (2005). Loss of Synaptonemal Complex Protein-1, a Synaptonemal Complex Protein, Contributes to the Initiation of Follicular Assembly in the Developing Rat Ovary. *Endocrinology*, 146(12), 5267-5277. <https://doi.org/10.1210/en.2005-0965>
- Paredes, J. A., Ezerskyte, M., Bottai, M., & Dreij, K. (2017). Transcriptional mutagenesis reduces splicing fidelity in mammalian cells. *Nucleic Acids Research*, 45(11), 6520-6529. <https://doi.org/10.1093/nar/gkx339>
- Parodi, D. A., Sjarif, J., Chen, Y., & Allard, P. (2015). Reproductive toxicity and meiotic dysfunction following exposure to the pesticides Maneb, Diazinon and Fenarimol. *Toxicology Research*, 4(3), 645-654. <https://doi.org/10.1039/C4TX00141A>
- Perillo, B., Ombra, M. N., Bertoni, A., Cuozzo, C., Sacchetti, S., Sasso, A., Chiariotti, L., Malorni, A., Abbondanza, C., & Avvedimento, E. V. (2008). DNA Oxidation as Triggered by H3K9me2 Demethylation Drives Estrogen-Induced Gene Expression. *Science*, 319(5860), 202-206. <https://doi.org/10.1126/science.1147674>
- Schmid, R., Grellscheid, S. N., Ehrmann, I., Dalgliesh, C., Danilenko, M., Paronetto, M. P., Pedrotti, S., Grellscheid, D., Dixon, R. J., Sette, C., Eperon, I. C., & Elliott, D. J. (2013). The splicing landscape is globally reprogrammed during male meiosis. *Nucleic Acids Research*, 41(22), 10170-10184. <https://doi.org/10.1093/nar/gkt811>
- Shin, N., Cuenca, L., Karthikraj, R., Kannan, K., & Colaiácovo, M. P. (2019). Assessing effects of germline exposure to environmental toxicants by high-throughput screening in *C. elegans*. *PLoS Genetics*, 15(2), e1007975. <https://doi.org/10.1371/journal.pgen.1007975>
- Soh, Y. Q. S., Junker, J. P., Gill, M. E., Mueller, J. L., van Oudenaarden, A., & Page, D. C. (2015). A Gene Regulatory Program for Meiotic Prophase in the Fetal Ovary. *PLoS Genetics*, 11(9), e1005531. <https://doi.org/10.1371/journal.pgen.1005531>
- Spiller, C., & Bowles, J. (2019). Sexually dimorphic germ cell identity in mammals. In *Current Topics in Developmental Biology* (Vol. 134, p. 253-288). Elsevier. <https://doi.org/10.1016/bs.ctdb.2019.01.011>
- Susiarjo, M., Hassold, T. J., Freeman, E., & Hunt, P. A. (2007). Bisphenol A Exposure In Utero Disrupts Early Oogenesis in the Mouse. *PLoS Genetics*, 3(1), e5. <https://doi.org/10.1371/journal.pgen.0030005>
- Susiarjo, M., Sasson, I., Mesaros, C., & Bartolomei, M. S. (2013). Bisphenol A Exposure Disrupts Genomic Imprinting in the Mouse. *PLoS Genetics*, 9(4), e1003401. <https://doi.org/10.1371/journal.pgen.1003401>
- Trautmann, E., Guerquin, M.-J., Duquenne, C., Lahaye, J.-B., Habert, R., & Livera, G. (2008). Retinoic acid prevents germ cell mitotic arrest in mouse fetal testes. *Cell Cycle*, 7(5), 656-664. <https://doi.org/10.4161/cc.7.5.5482>
- Tu, Z., Mu, X., Chen, X., Geng, Y., Zhang, Y., Li, Q., Gao, R., Liu, T., Wang, Y., & He, J. (2019). Dibutyl phthalate exposure disrupts the progression of meiotic prophase I by interfering with homologous recombination in fetal mouse oocytes. *Environmental Pollution (Barking, Essex: 1987)*, 252(Pt A), 388-398. <https://doi.org/10.1016/j.envpol.2019.05.107>

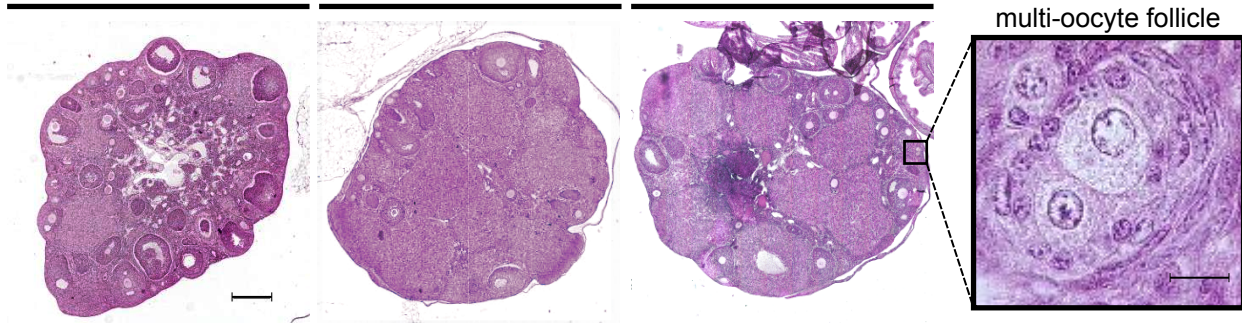
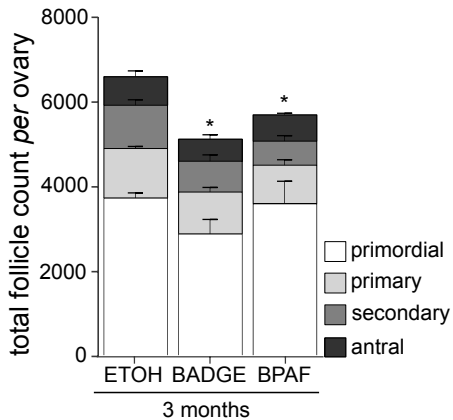
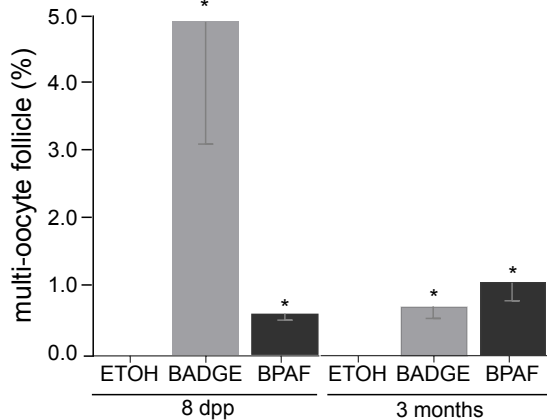
- Wang, J., Tian, G. G., Zheng, Z., Li, B., Xing, Q., & Wu, J. (2019). Comprehensive Transcriptomic Analysis of Mouse Gonadal Development Involving Sexual Differentiation, Meiosis and Gametogenesis. *Biological Procedures Online*, 21, 20. <https://doi.org/10.1186/s12575-019-0108-y>
- Wang, L., Xue, J., & Kannan, K. (2015). Widespread occurrence and accumulation of bisphenol A diglycidyl ether (BADGE), bisphenol F diglycidyl ether (BFDGE) and their derivatives in human blood and adipose fat. *Environmental Science & Technology*, 49(5), 3150-3157. <https://doi.org/10.1021/acs.est.5b00096>
- Wang, S., Hassold, T., Hunt, P., White, M. A., Zickler, D., Kleckner, N., & Zhang, L. (2017). Inefficient Crossover Maturation Underlies Elevated Aneuploidy in Human Female Meiosis. *Cell*, 168(6), 977-989.e17. <https://doi.org/10.1016/j.cell.2017.02.002>
- Wang, T., Han, J., Duan, X., Xiong, B., Cui, X.-S., Kim, N.-H., Liu, H.-L., & Sun, S.-C. (2016). The toxic effects and possible mechanisms of Bisphenol A on oocyte maturation of porcine *in vitro*. *Oncotarget*, 7(22). <https://doi.org/10.18632/oncotarget.8689>
- Wang, W., Hafner, K. S., & Flaws, J. A. (2014). In utero bisphenol A exposure disrupts germ cell nest breakdown and reduces fertility with age in the mouse. *Toxicology and Applied Pharmacology*, 276(2), 157-164. <https://doi.org/10.1016/j.taap.2014.02.009>
- Yamaguchi, S., Hong, K., Liu, R., Shen, L., Inoue, A., Diep, D., Zhang, K., & Zhang, Y. (2012). Tet1 controls meiosis by regulating meiotic gene expression. *Nature*, 492(7429), 443-447. <https://doi.org/10.1038/nature11709>
- Yu, G., Wang, L.-G., Han, Y., & He, Q.-Y. (2012). clusterProfiler: An R Package for Comparing Biological Themes Among Gene Clusters. *OMICS: A Journal of Integrative Biology*, 16(5), 284-287. <https://doi.org/10.1089/omi.2011.0118>
- Yu, M., Xu, Y., Li, M., Li, D., Lu, Y., Yu, D., & Du, W. (2018). Bisphenol A accelerates meiotic progression in embryonic chickens via the estrogen receptor  $\beta$  signaling pathway. *General and Comparative Endocrinology*, 259, 66-75. <https://doi.org/10.1016/j.ygcen.2017.11.004>
- Zhang, H.-Q., Zhang, X.-F., Zhang, L.-J., Chao, H.-H., Pan, B., Feng, Y.-M., Li, L., Sun, X.-F., & Shen, W. (2012). Fetal exposure to bisphenol A affects the primordial follicle formation by inhibiting the meiotic progression of oocytes. *Molecular Biology Reports*, 39(5), 5651-5657. <https://doi.org/10.1007/s11033-011-1372-3>
- Zhang, M., Dai, X., Lu, Y., Miao, Y., Zhou, C., Cui, Z., Liu, H., & Xiong, B. (2017). Melatonin protects oocyte quality from Bisphenol A-induced deterioration in the mouse. *Journal of Pineal Research*, 62(3), e12396. <https://doi.org/10.1111/jpi.12396>
- Zhang, T., Li, L., Qin, X.-S., Zhou, Y., Zhang, X.-F., Wang, L.-Q., De Felici, M., Chen, H., Qin, G.-Q., & Shen, W. (2014). Di-(2-ethylhexyl) phthalate and bisphenol A exposure impairs mouse primordial follicle assembly in vitro: DEHP and BPA Impairs Mouse Primordial Follicle Assembly. *Environmental and Molecular Mutagenesis*, 55(4), 343-353. <https://doi.org/10.1002/em.21847>
- Zhang, T., Zhou, Y., Li, L., Zhao, Y., De Felici, M., Reiter, R. J., & Shen, W. (2018). Melatonin protects prepuberal testis from deleterious effects of bisphenol A or diethylhexyl phthalate by preserving H3K9 methylation. *Journal of Pineal Research*, 65(2), e12497. <https://doi.org/10.1111/jpi.12497>

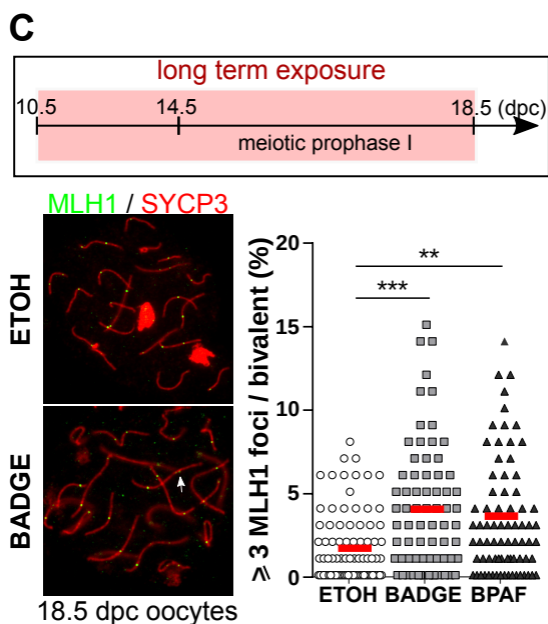
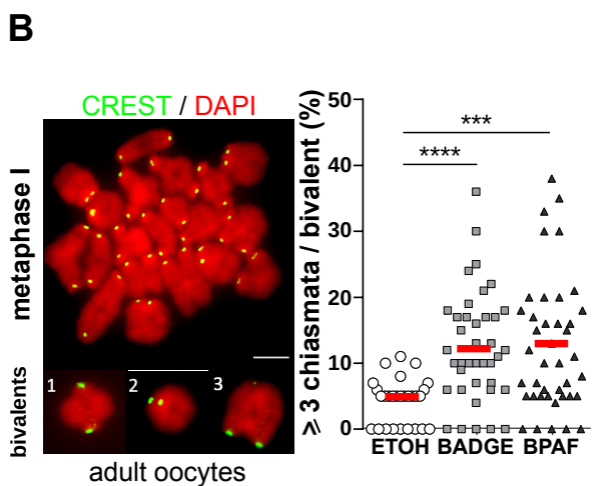
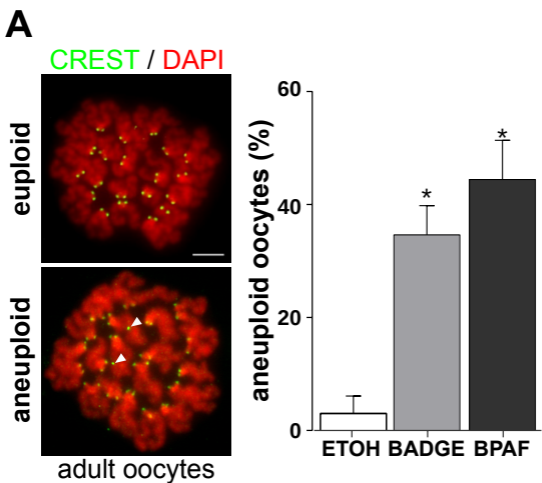
**A**

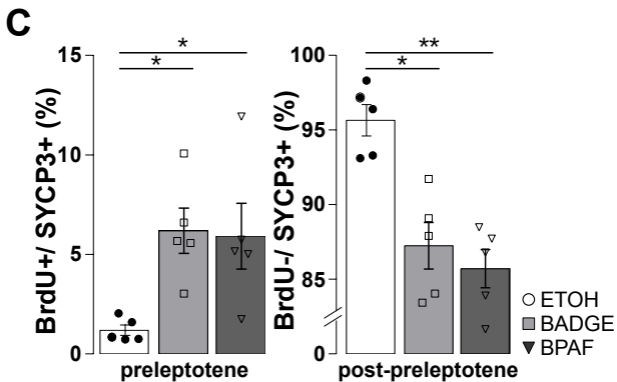
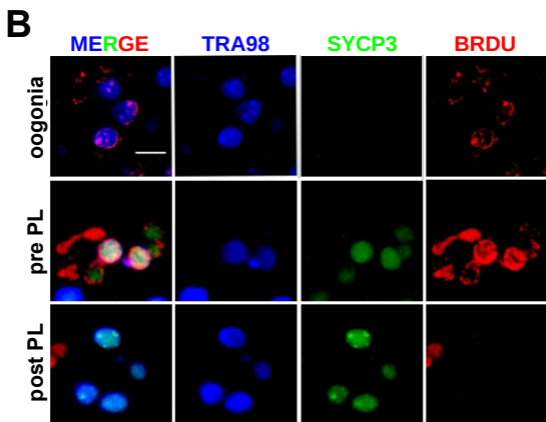
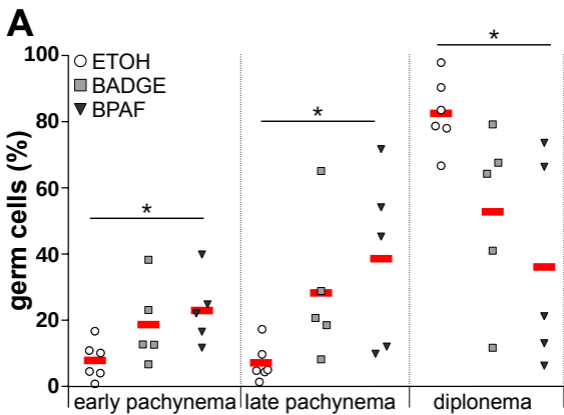
ETOH

BADGE

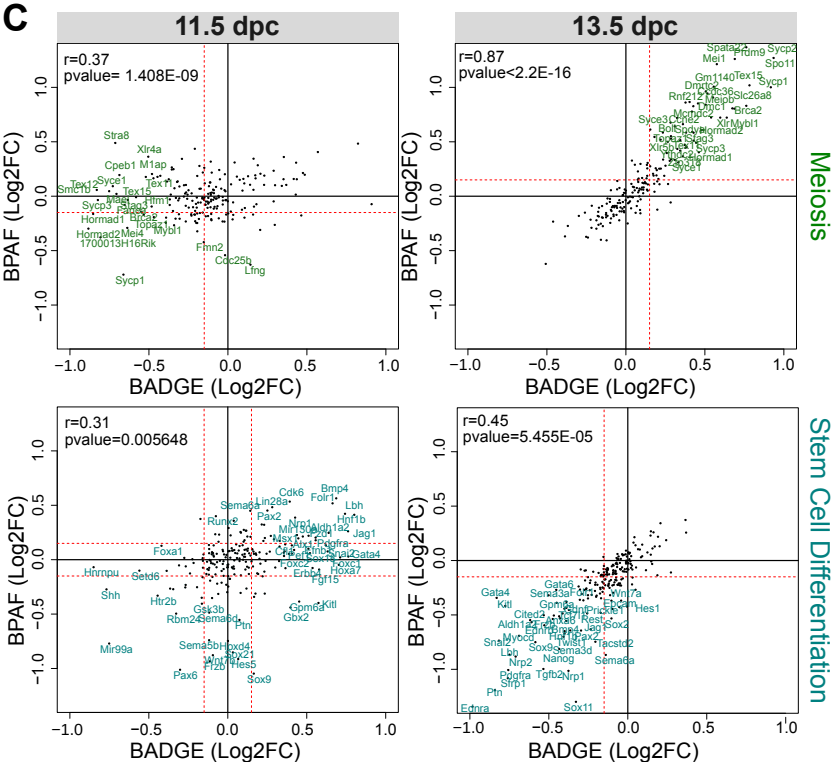
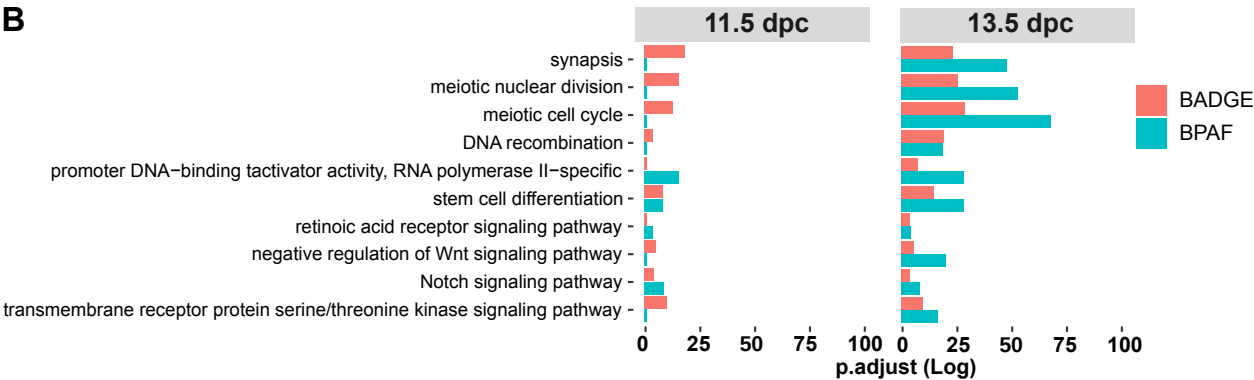
BPAF

**B****C**

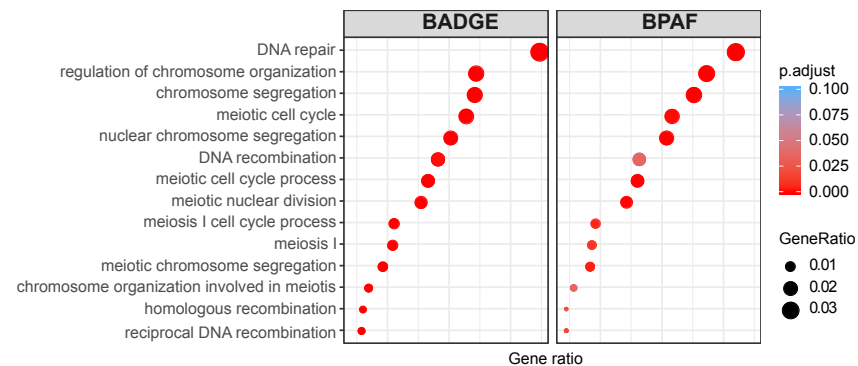




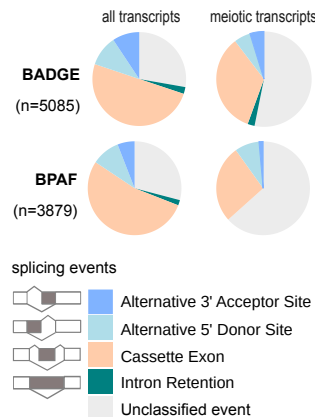
	11.5dpc		13.5dpc	
	BADGE	BPAF	BADGE	BPAF
<b>DEG</b> (LFC>0.5, pvalue <0.05)	<b>1817</b>	<b>733</b>	<b>886</b>	<b>1376</b>
<i>upregulated</i>	802 (44.2%)	243 (34.6%)	640 (72.2%)	846 (61.4%)
<i>downregulated</i>	1015 (55.8 %)	490 (65.4%)	247 (27.8%)	528 (38.6%)



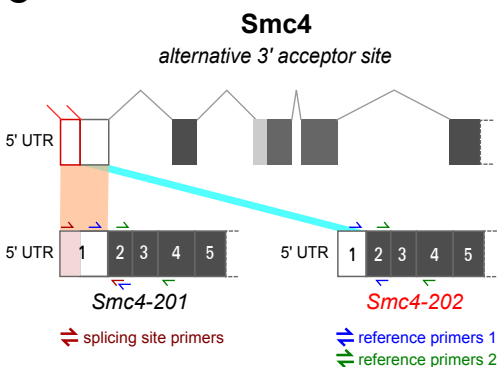
A



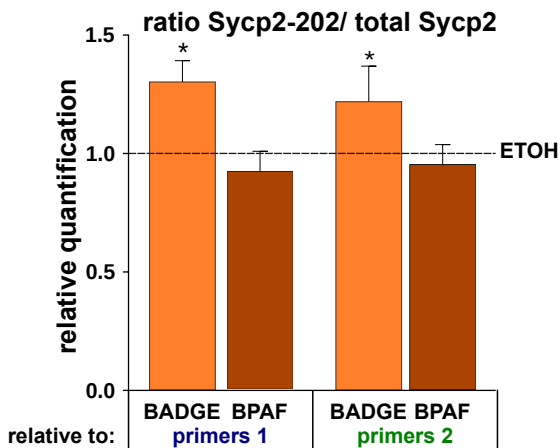
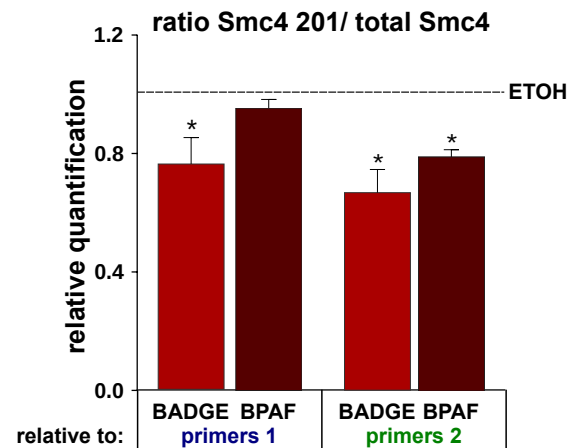
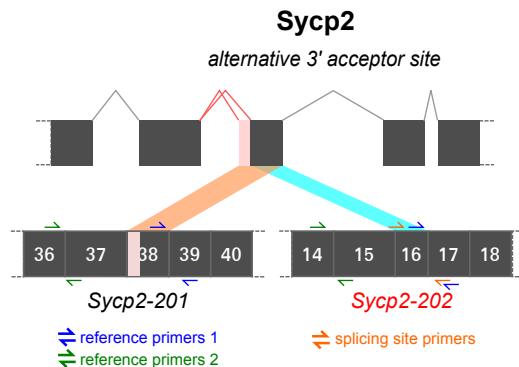
B

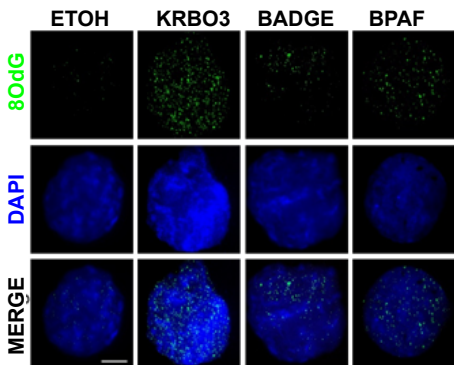
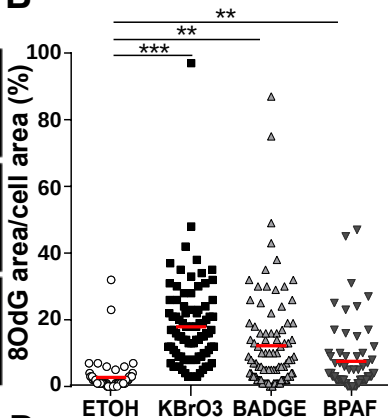
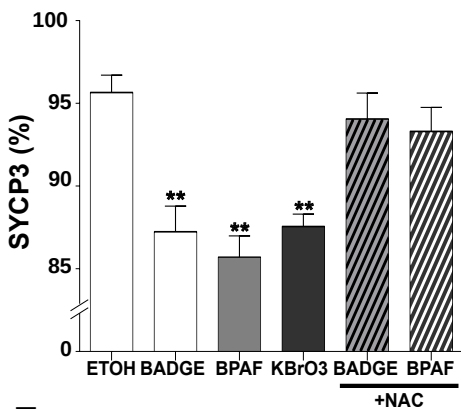
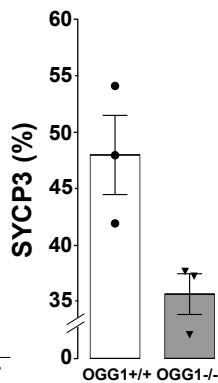
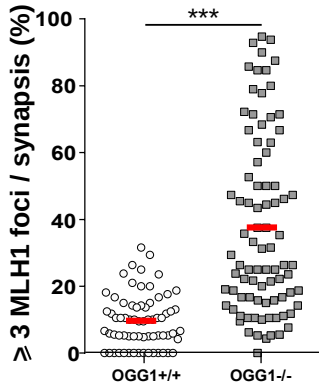


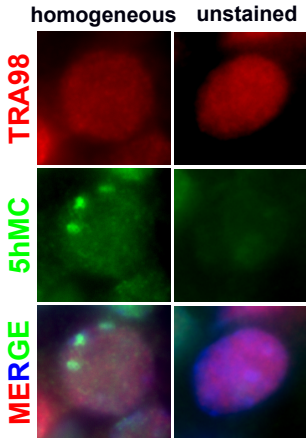
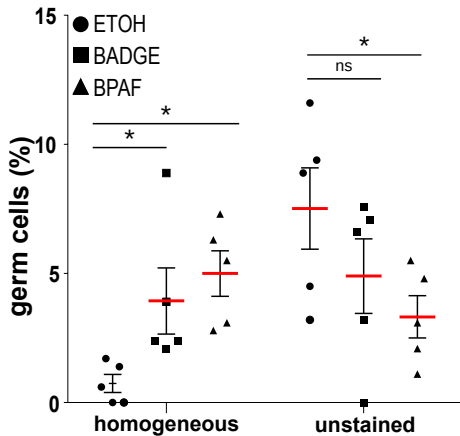
C

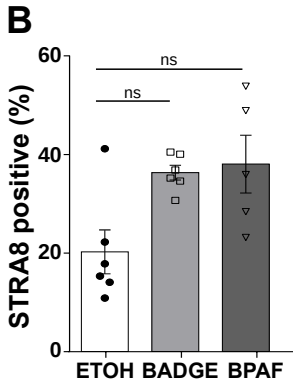
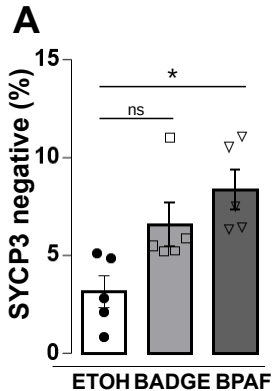


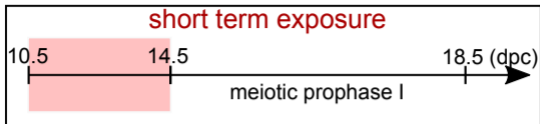
D



**A****B****C****D****E**

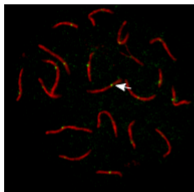
**A****B**



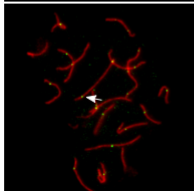


MLH1 / SYCP3

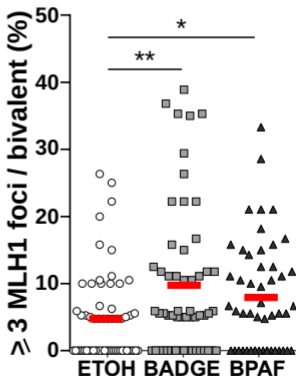
ETOH



BADGE

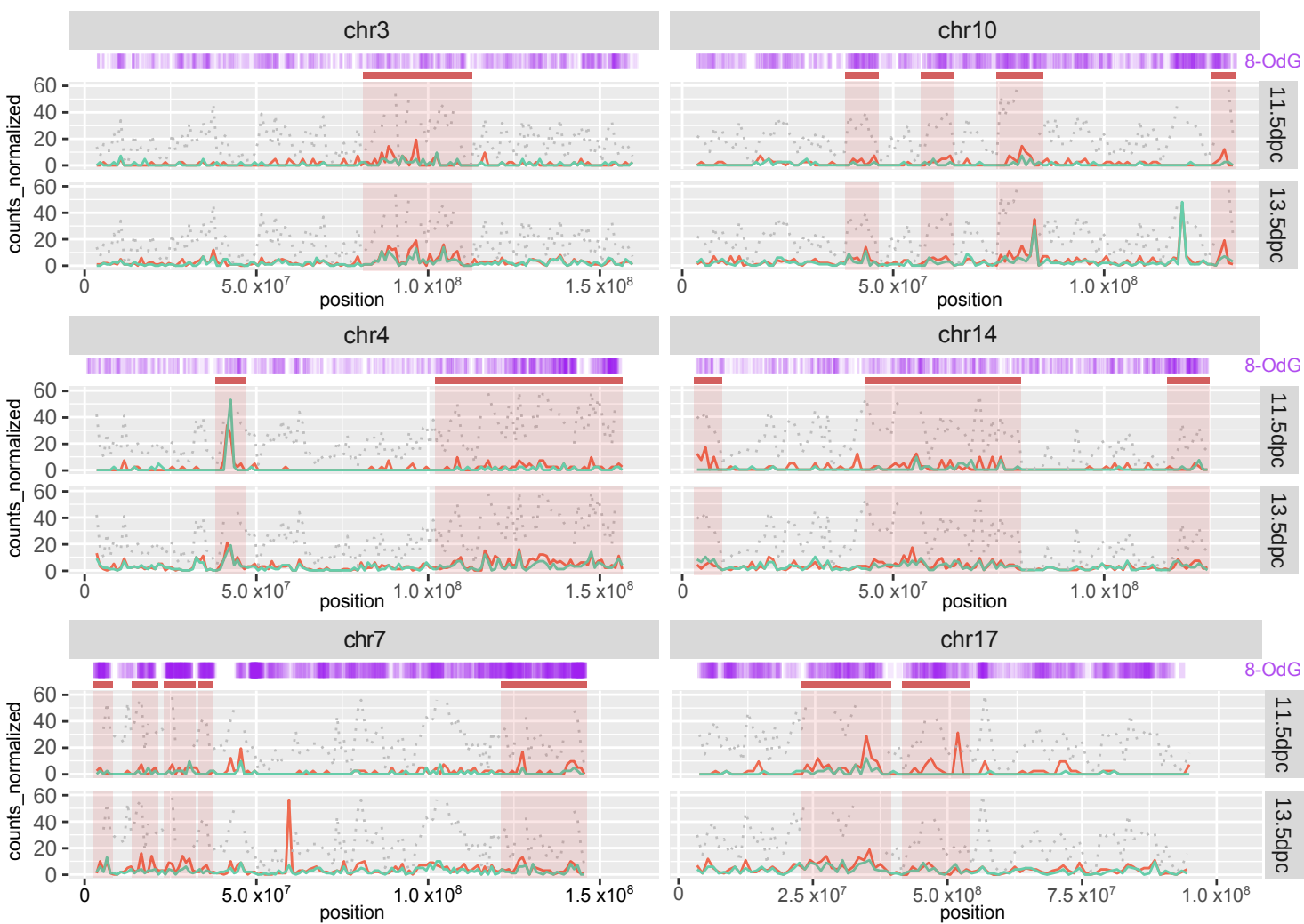


18.5 dpc oocytes

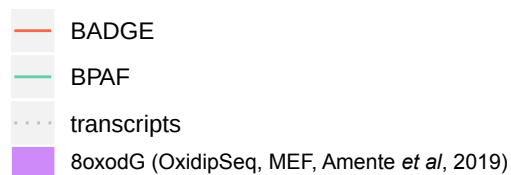








condition



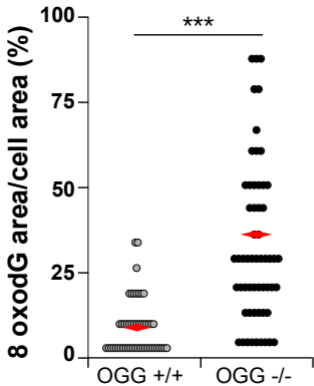


Table 1: List of common genes between BADGE and BPAF conditions showing an alternative splicing relative to control germ cell.

Go term	Differentially Spliced genes count (adj <i>pvalue</i> )	Common genes between bisphenols	
		%	common genes
Chromosome Segregation (GO:0007059)	105 (BADGE ; <i>pvalue</i> 9 x10 <sup>-8</sup> )  85 (BPAF; <i>pvalue</i> 2 x10 <sup>-6</sup> )	46 % (BADGE)  56% (BPAF)	<i>Smc4, Espl1, Mms19, Srpk1, Cit, Ccne1, Psrc1, Bub1b, Pttg1, Kif4, Mlh1, Dync1h1, Zw10, Zwint, Cep63, Hecw2, Spag5, Pogz, Pum1, Mcmdc2, Top2b, Bub1, Setdb2, Anapc1, Atm, Pibf1, Msto1, Mau2, Cdc20, Ndc1, Fancd2, Usp9x, Top3b, Tpr, Ago4, Ncapd3, Sun1, Cenph, Nipbl, Ddx11, Hira, Csnk2a1, Lrrk1, Smc1b, Ino80, Dmc1, Hfm1</i>
DNA repair (GO:0006281)	151 (BADGE; <i>pvalue</i> : 5 x10 <sup>-10</sup> )  108 (BPAF; <i>pvalue</i> : 7 x10 <sup>-06</sup> )	44 % (BADGE)  61 % (BPAF)	<i>Nhej1, Nabp1, Pold2, Gins4, Wrn, Uchl5, Smc4, Hdac9, Npas2, Usp47, Mms19, Prkdc, Pms2, Fanci, Pif1, Upf1, Pttg1, Rad51, Mlh1, Cdc45, Kdm2a, Usp3, Otub1, Abl1, Dclre1a, Shprh, Parp9, Cep164, Neil1, Marf1, Rbm17, Mcmdc2, Npm1, Top2b, Taok3, Ticrr, Cdc5l, Supt16, Xpc, Atm, Rad52, Uimc1, Poli, Ube2t, Taok1, Rbbp8, Fancd2, Setx, Sprtn, Ercc6l2, Gtf2h1, Nipb, Atr, Alkbh1, Ddx11, Usp28, Eya1, Rtel1, Rif1, Rev1, Cdc7, Ino80, Dmc1, Huwe1, Helq</i>
Nuclear Chromosome Segregation (GO:0098813)	88 (BADGE; <i>pvalue</i> : 3 x10 <sup>-07</sup> )  70 (BPAF; <i>pvalue</i> : 12 x10 <sup>-05</sup> )	45 % (BADGE)  57 % (BPAF)	<i>Smc4, Espl1, Cit, Ccne1, Psrc1, Bub1b, Pttg1, Kif4, Mlh1, Dync1h1, Zw10, Zwint, Cep63, Hecw2, Spag5, Pogz, Mcmdc2, Top2b, Bub1, Anapc1, Atm, Pibf1, Msto1, Mau2, Cdc20, Ndc1, ancd2, Tpr, Ago4, Ncapd3, Sun1, Nipbl, Ddx11, Hira, Lrrk1, Smc1b, Ino80, Dmc1, Hfm1</i>
DNA Recombination (GO:0006310)	79 (BADGE, <i>pvalue</i> < 0.001)  5 (BPAF, <i>pvalue</i> : 0.04)	40 % (BADGE)  58 % (BPAF)	<i>Cntd1, Nabp1, Gins4, Ubr2, Wrn, Uchl5, Rag1, Mms19, Prkdc, Pms2, Pif1, Rad51, Mlh1, Cdc45, Cep63, Thoc1, Mcmdc2, Top2b, Atm, Rad52, Rbbp8, Setx, Psmc3ip, Nipbl, Rtel1, Rif1, Cdc7, Ino80, Dmc1, Hfm1, Gm960, Helq</i>
Meiotic Cell Cycle process (GO:0051321)	99 (BADGE; <i>pvalue</i> : 2 x10 <sup>-06</sup> )  73 (BPAF; <i>pvalue</i> <0.001)	11 % (BADGE)  15% (BPAF)	<i>Tdrd9, Cntd1, Topaz1, Ubr2, Smc4, Espl1, Ccne1, Bub1b, Pttg1, Rad51, Mlh1, Marf1, Cep63, Plcb1, Nsun2, Mcmdc2, Top2b, Bub1, Atm, Cdc20, Ndc1, Fancd2, Psmc3ip, Ago4, Ncapd3, Sun1, Lrrk1, Aspm, Dmc1, Hfm1, Gm960, Sycp2</i>

Table 2: Splicing event EEJ: one exon-exon junction was covered by probes, E: one exon was covered by probes. Only PSRs are assigned Event Estimation Name

Gene Symbol	Probes			Splicing event estimation name	Splicing pvalue ( $p \leq 0.01$ )	
	target	location	Isoform name		BADGE	BPAF
<i>Ago4</i>	EEJ	Exons 11-12	Ago4-201	-	ns	0.0028
	EEJ	Exons 9-10	Ago4-201	-	0.0093	ns
<i>Aspm</i>	EEJ	Exons 1-2	Aspm-201	-	0.0007	ns
	E	Exon 18	Aspm-201	ND	ns	0.0044
<i>Atm</i>	EEJ	Exons 56-57	Atm-201	-	0.0061	0.0093
	EEJ	Exons 52-53	Atm-201	-	ns	0.0061
	EEJ	Exons 47-48	Atm-201	-	0.0039	ns
	EEJ	Exons 49-50	Atm-201	-	0.002	0.0017
	E	Exon 29	Atm-201	Cassette Exon	0.01	ns
<i>Bub1b</i>	EEJ	Exons 9-10	Bub1-201	-	0.0002	0.0044
	E	Exon1	Bub1-203	Alt 3' Acceptor Site	ns	0.0064
<i>Ccne1</i>	EEJ	Exons 6-7	Ccne-201	-	ns	0.0026
	E	Exon 1	Ccne-201	Cassette Exon	0.0035	ns
<i>Cdc7</i>	EEJ	Exons 6-8	Cdc7-201	-	0.0044	0.0366
<i>Cdc20</i>	EEJ	Exons 6-7	Cdc20-201	-	0.0041	ns
	E	Exon 1	Cdc20-201	Cassette Exon	ns	0.004
<i>Cdc45</i>	EEJ	Exons 19-20	Cdc45-201	-	ns	0.0089
	EEJ	Exons 11-12	Cdc45-201	-	0.009	ns
	EEJ	Exons 1-2	Cdc45-201	-	0.0094	ns
<i>Cep63</i>	E	Exon 7	Cep63-201	Cassette Exon	0.0024	0.0047
<i>Cntd1</i>	E	Exon 1 (-5')	Cntd1-201	Cassette Exon	ns	0.007
	E	Exon 1 (-3')	Cntd1-201	Cassette Exon	ns	0.0074
	E	Exon 3	Cntd1-203	Cassette Exon	0.0012	ns
<i>Dmc1</i>	EEJ	Exons 9-10	Dmc1-201	-	0.0004	0.0069
	EEJ	Exons 7-8	Dmc1-201	-	0.0013	ns
<i>Espl1</i>	EEJ	Exons 1-2	Espl1-201	-	0.003	0.0039
<i>Fancd2</i>	EEJ	Exons 22-23	Fancd2-201	-	0.0019	0.0088
	EEJ	Exons 31-32	Fancd2-201	-	0.0096	ns
<i>Gins4</i>	EEJ	Exons 2-3	Gins4-201	-	0.0061	ns
	E	Exon 8	Gins4-201	Alt 5' Donor Site	ns	0.0045
<i>Gm960 (Top6bl)</i>	EEJ	Exons 3-4	Gm960-201	-	ns	0.0039
	E	Exon 12	Gm960-202	Cassette Exon	0.0033	ns
	E	Exon 11	Gm960-202	Cassette Exon	0.0076	ns
<i>Helq</i>	EEJ	Exons 16-17	Helq-201	-	0.0000157	0.0038
	EEJ	Exons 12-13	Helq-201	-	0.0088	ns
<i>Hfm1</i>	EEJ	Exons 7-8	Hfm1-201	-	ns	0.0076
	E	Exon 22	Hfm1-201	Cassette Exon	0.0031	ns
	E	Exon 21	Hfm1-201	Cassette Exon	0.0087	ns
	E	Exon 4	Hfm1-204	Cassette Exon	0.0005	ns
<i>Ino80e</i>	EEJ	Exons 2-3	Ino80e-203	-	0.0007	0.0034
<i>Lrrk1</i>	E	Exon 28	Lrrk1-201	Cassette Exon	0.0077	0.0042
<i>Marf1</i>	EEJ	Exons 24-25	Marf1-201	-	ns	0.0084

	EEJ	Exons 9-10	Marf1-201	-	0.0023	0.0069
<i>Mcmdc2</i>	E E E	Exon 10 Exon 14 Exon 16	Mcmdc2-201 Mcmdc2-203 Mcmdc2-204	- Cassette Exon Alt 5' Donor Site	ns 0.0047 0.0018	0.0096 n ns
<i>Mlh1</i>	EEJ E E	Exons 15-17 Exon 18 Exon 18	Mlh1-201 Mlh1-206 Mlh1-201	- ND ND	ns 0.0056 0.0035	0.0091 ns ns
<i>Mms19</i>	EEJ E E E	Exons 4-6 Exon 28 Intron 6 Exon 6	Mms19-201 Mms19-201 Mms19-201 Mms19-201	- Cassette Exon Intron Retention Cassette Exon	0.0008 ns 0.0066 0.0094	0.007 0.0022 0.0021 ns
<i>Nabp1</i>	EEJ E E	Exons 5-6 Exon 1 Exon 6	Nabp1-204 Nabp1-208 Nabp1-201	- Alt 5' Donor Site ND	0.0088 0.004 ns	ns ns 0.0056
<i>Ncapd3</i>	EEJ E E E	Exons 29-30 Exon 4 Exon 26 Exon 29	Ncapd3-201 Ncapd3-201 Ncapd3-201 Ncapd3-201	- Cassette Exon Cassette Exon Cassette Exon	ns 0.0069 0.0047 0.0041	0.0065 ns ns ns
<i>Ndc1</i>	EEJ	Exons 1-2	Ndc1-205	-	0.0018	0.0032
<i>Nipbl</i>	EEJ E E	Exons 25-26 Exon 28 Exon 16	Nipbl-201 Nipbl-201 Nipbl-201	- Cassette Exon Cassette Exon	0.001 ns ns	ns 0.004 0.0055
<i>Nsun2</i>	EEJ EEJ	Exons 7-8 Exons 1-2	Nsun2-201 Nsun2-203	- -	0.002 ns	ns 0.0045
<i>Plcb1</i>	E	Exon 32	Plcb1-201	Cassette Exon	0.0017	0.0079
<i>Prkdc</i>	EEJ	Exons 52-53	Prkdc-201	-	0.0039	0.0079
<i>Psmc3ip</i>	EEJ	Exons 2-3	Psmc3ip-201	-	0.0025	0.0059
<i>Pttg1</i>	E	Exon 1	Pttg1-201	Alt 5' Donor Site	0.0026	0.0026
<i>Rad51</i>	EEJ EEJ	Exons 1-2 Exons 7-8	Rad51-201 Rad51-201	- -	0.0064 0.0023	ns 0.0012
<i>Rag1</i>	E E	Exon 6 Exon 1	Rag1-201 Rag1-207	Cassette Exon Cassette Exon	0.01 ns	ns 0.0085
<i>Rif1</i>	EEJ E E E	Exons 24-25 Exon 5 Exon 18 Exon 22	Rif1-201 Rif1-201 Rif1-201 Rif1-201	- Cassette Exon Cassette Exon ND	0.003 0.0068 ns ns	0.0058 ns 0.0083 0.0027
<i>Rbbp8</i>	EEJ	Exons 15-16	Rbbp8-201	-	0.0000841	0.0002
<i>Rtel1</i>	EEJ E	Exons 6-7 Exon 18	Rtel1-201 Rtel1-201	- Cassette Exon	ns 0.005	0.0025 ns
<i>Setx</i>	EEJ E	Exons 17-18 Exon 4	Setx-201 Setx-201	- Cassette Exon	0.0082 0.0067	ns 0.0041
<i>Smc4</i>	EEJ EEJ E E	Exons 9-10 Exons 19-20 Exon 1 Exon 8	Smc4-201 Smc4-201 Smc4-201 Smc4-201	- - Alt 3' Acceptor Site Alt 5' Donor Site	ns ns 0.0039 0.0034	0.0072 0.0061 0.0024 0.0049
<i>Sycp2</i>	EEJ E E	Exons 36-37 Exon 38 Exon 36	Sycp2-201 Sycp2-201 Sycp2-201	- Alt 3' Acceptor Site Cassette Exon	0.0022 0.0027 0.0000384	ns ns 0.0003

<i>Sun1</i>	EEJ	Exons 8-10	Sun1-201	-	0.0094	ns
	EEJ	Exons 13-14	Sun1-201	-	0.0089	ns
	EEJ	Exons 2-3	Sun1-218	-	0.0063	ns
	EEJ	Exons 6-8	Sun1-201	-	0.0055	ns
	E	Exon 1	Sun1-215	ND	0.0003	0.01
	E	Exon 4	Sun1-201	Alt 3' Acceptor Site	0.0094	ns
	E	Exon 15	Sun1-201	Cassette Exon	0.0076	ns
	E	Exon 17	Sun1-201	Cassette Exon	0.0007	0.01
	E	Exon 18	Sun1-201	Alt 3' Acceptor Site	0.0081	ns
	E	Exon 23	Sun1-201	Alt 5' Donor Site	ns	0.01
<i>Tdrd9</i>	E	Exon 5	Tdrd9-201	Cassette Exon	ns	0.0026
	E	Exon 6	Tdrd9-201	Cassette Exon	ns	0.0077
	E	Exon 24	Tdrd9-201	Cassette Exon	0.005	ns
<i>Thoc1</i>	EEJ	Exons 3-4	Thoc1-201	-	ns	0.01
	E	Exon 7	Thoc1-201	Cassette Exon	0.0054	ns
<i>Top2b</i>	EEJ	Exons 6-7	Top2b-201	-	ns	0.009
	EEJ	Exons 22-23	Top2b-201	-	0.0096	ns
	EEJ	Exons 25-26	Top2b-201	-	0.008	ns
<i>Topaz</i>	EEJ	Exons 4-5	Topaz1-201	-	0.0038	ns
	EEJ	Exons 9-10	Topaz1-201	-	ns	0.0047
	E	Exon 10	Topaz1-201	Cassette Exon	0.0014	ns
<i>Ubr2</i>	E	Exon 1	Ubr-201	ND	0.007	ns
	EEJ	Exons 44-45	Ubr-201	-	ns	0.005
	EEJ	Exons 27-28	Ubr-201	-	ns	0.0029
	E	Exon 5	Ubr-201	Cassette Exon	ns	0.0075
	E	Exon 1	Ubr-205	Intron Retention	0.0074	ns
<i>Uchl5</i>	EEJ	Exons 1-2	Uchl5-201	-	0.0083	ns
	E	Exon 11	Uchl5-201	Alt 5' Donor Site	ns	0.0008
<i>Wrm</i>	EEJ	Exons 12-13	Wrm-201	-	0.0061	ns
	E	Exon 21	Wrm-201	Cassette Exon	ns	0.0057